AD-A123 683 GROUND RESPONSE IN ALLUVIAL BASINS DUE TO SEISMIC DISTURBANCES(U) COLUMBIA UNIV NEW YORK J T KUO ET AL. 01 AUG 82 SCIENTIFIC-1 AFGL-TR-82-0279 F19628-81-K-0012 1/1

UNCLASSIFIED F/G 8/11 NL

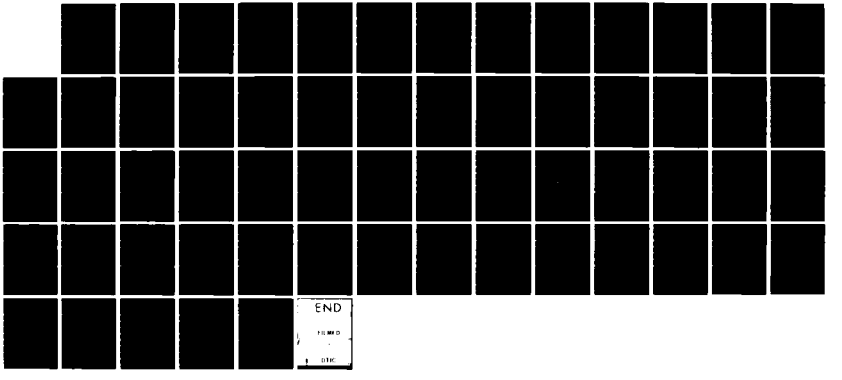

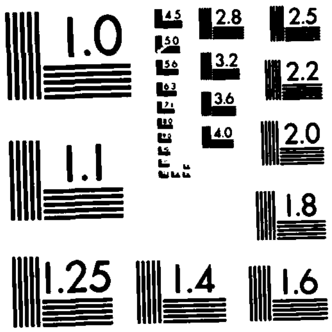

MICROCOPY RESOLUTION TEST CHART
NATIONAL BUREAU OF STANDARDS-1963-A

(12)

AFGL-TR-82-0279

GROUND RESPONSE IN ALLUVIAL BASINS DUE TO SEISMIC DISTURBANCES

John T. Kuo
Yu-Chiung Teng

Columbia University
New York, New York 10027

Scientific Report No. 1

1 August 1982

Approved for public release; distribution unlimited

AIR FORCE GEOPHYSICS LABORATORY
AIR FORCE SYSTEMS COMMAND
UNITED STATES AIR FORCE
HANSCOM AFB, MASSACHUSETTS 01731

Unclassified

SECURITY CLASSIFICATION OF THIS PAGE (When Data Entered)

REPORT DOCUMENTATION PAGE		READ INSTRUCTIONS BEFORE COMPLETING FORM
1. REPORT NUMBER AFGL-TR-82-0279	2. GOVT ACCESSION NO. AD-A123683	3. RECIPIENT'S CATALOG NUMBER
4. TITLE (and Subtitle) Ground Response in Alluvial Basins due to Seismic Disturbances		5. TYPE OF REPORT & PERIOD COVERED Scientific Report No. 1 26 March 1981 to 30 April 82 6. PERFORMING ORG. REPORT NUMBER
7. AUTHOR(s) John T. Kuo Yu-Chiung Teng		8. CONTRACT OR GRANT NUMBER(s) F19628-81-K-0012
9. PERFORMING ORGANIZATION NAME AND ADDRESS Columbia University New York, New York 10027		10. PROGRAM ELEMENT, PROJECT, TASK AREA & WORK UNIT NUMBERS 61102F 2309-G2-AH
11. CONTROLLING OFFICE NAME AND ADDRESS Air Force Geophysics Laboratory Hanscom AFB, MA 01731 Manager/John Cipar/LWH		12. REPORT DATE 1 August 1982 13. NUMBER OF PAGES 57
14. MONITORING AGENCY NAME & ADDRESS(if different from Controlling Office)		15. SECURITY CLASS. (of this report) Unclassified 15a. DECLASSIFICATION/DOWNGRADING SCHEDULE

16. DISTRIBUTION STATEMENT (of this Report)

Approved for public release;
Distribution unlimited.

17. DISTRIBUTION STATEMENT (of the abstract entered in Block 20, if different from Report)

18. SUPPLEMENTARY NOTES

19. KEY WORDS (Continue on reverse side if necessary and identify by block number)

Elastic Waves
Finite element Analysis
Seismic Ground Motion

20. ABSTRACT (Continue on reverse side if necessary and identify by block number)

This summarizes the first year's accomplishments under Contract F19628-81-K-0012. Our scientific accomplishments include systematically studying four finite element basin models for SH waves and two more complex basin models for elastic waves; and modifying the two-dimensional finite element computer code for SH waves and elastic waves. The non-reflecting boundaries have been introduced in finite element modeling. The method of Effective Excitation, the relative coordinates of the nodal points, and a restart back-up capability have been introduced into the computer codes.

DD FORM 1 JAN 73 1473

Unclassified

SECURITY CLASSIFICATION OF THIS PAGE (When Data Entered)

Contents

INTRODUCTION

In the first year of Contract F19628-81-K-0012, "Ground Response in Alluvial Basins Due to Seismic Disturbances," from March 26, 1981, to April 30, 1982, our research emphasis has been in the following two areas:

I. Solving the finite element basin models for elastic (P and S) waves, starting with simple basin models and then more complex basin models.

II. Modifying and improving our two-dimensional finite element computer codes (for elastic and SH waves):

   (a) implementing the non-reflecting boundaries;

   (b) introducing Effective Excitation (EE) method;

   (c) introducing the relative coordinates of the nodal points; and

   (d) introducing the restart and back-up capability.

SCIENTIFIC ACCOMPLISHMENTS

I. Finite Element Modeling of Basins.

(a) Simple Models for SH Waves

The following three simple basin models for SH waves have been investigated.

Model 1:

At the suggestion of Mr. J. Battis at AFGL, we first model an homogeneous truncated medium as shown in Fig. 1, with 500 quadrilateral finite elements. The model assumes shear velocity v_s = 2,900 m/sec, density ρ = 2.67 gm/cm^3; grid size $\Delta x = \Delta y$ = 85m. A uniform SH wave forcing function of the first derivative of a Gaussian function is loaded on the lower boundary AA' of the medium.

The synthetic seismograms of displacement u_z along the vertical planes OA and BC, with a sampling space Δx = 425m and time step Δt = 0.02 sec, are shown in Figs. 2 and 3. These two seismograms are exactly identical. Figs. 4 and 5 show the identical responses along the horizontal surfaces 00' and MM'. These expected identical responses, due to a uniform external forcing function along AA', assure the correctness of the finite element results. In Figs. 2 and 3, the direct and reflected pulses from AA' and 00' can be clearly identified.

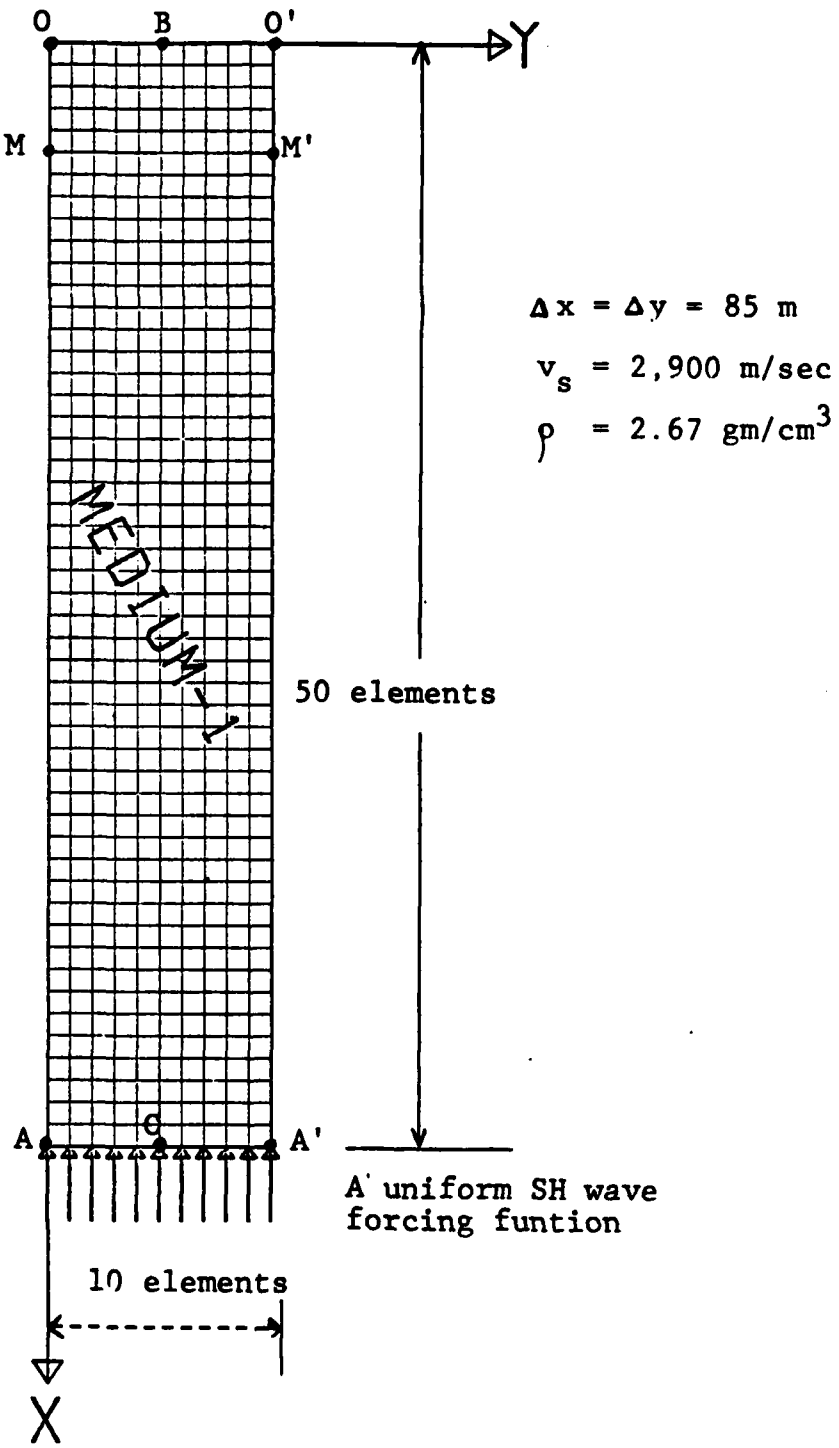

Figure 1. Finite Element Model 1.

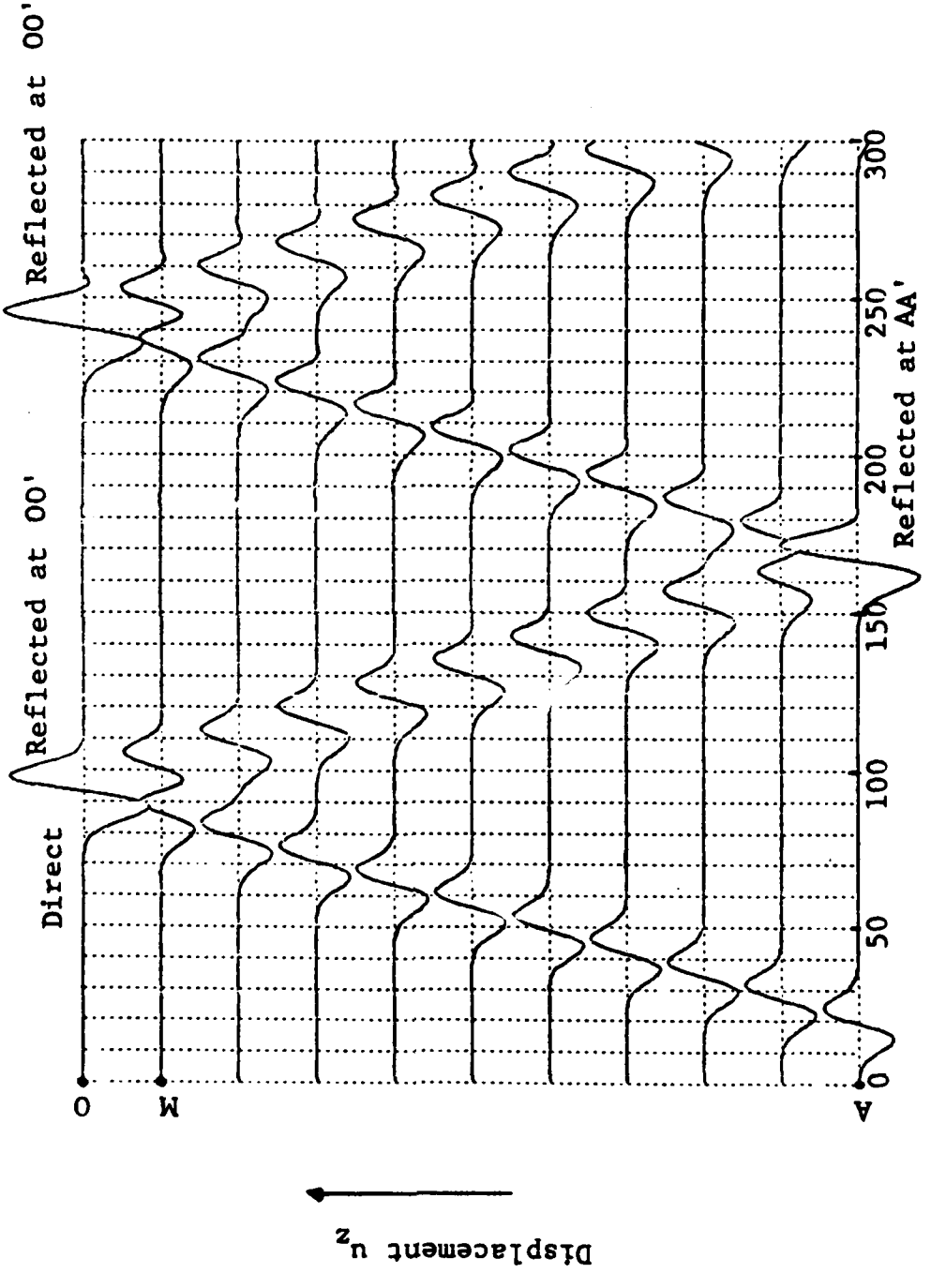

Figure 2. Synthetic Seismogram Along Vertical Plane OA For Model 1.

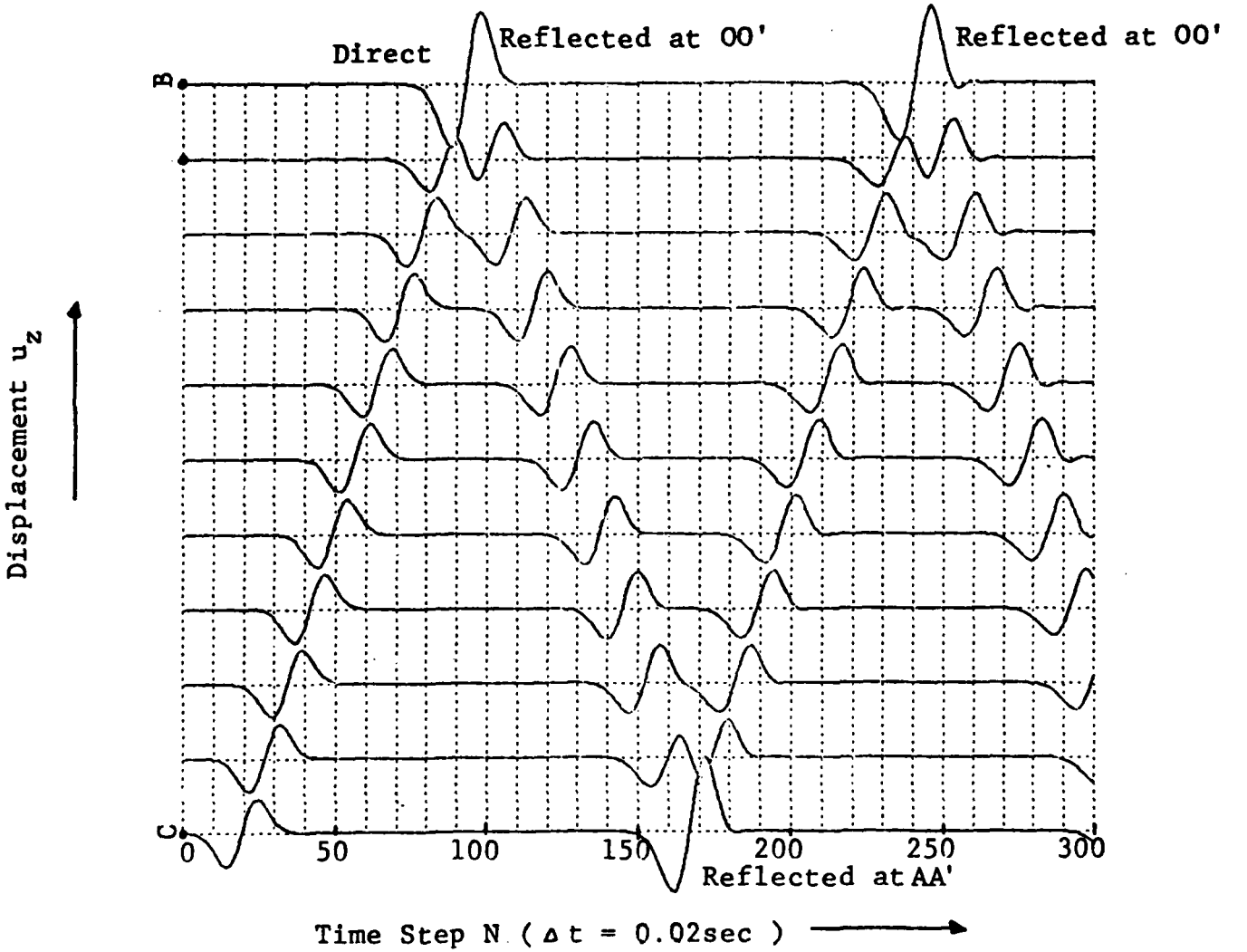

Figure 3. Synthetic Seismogram Along Vertical Plane BC For Model 1.

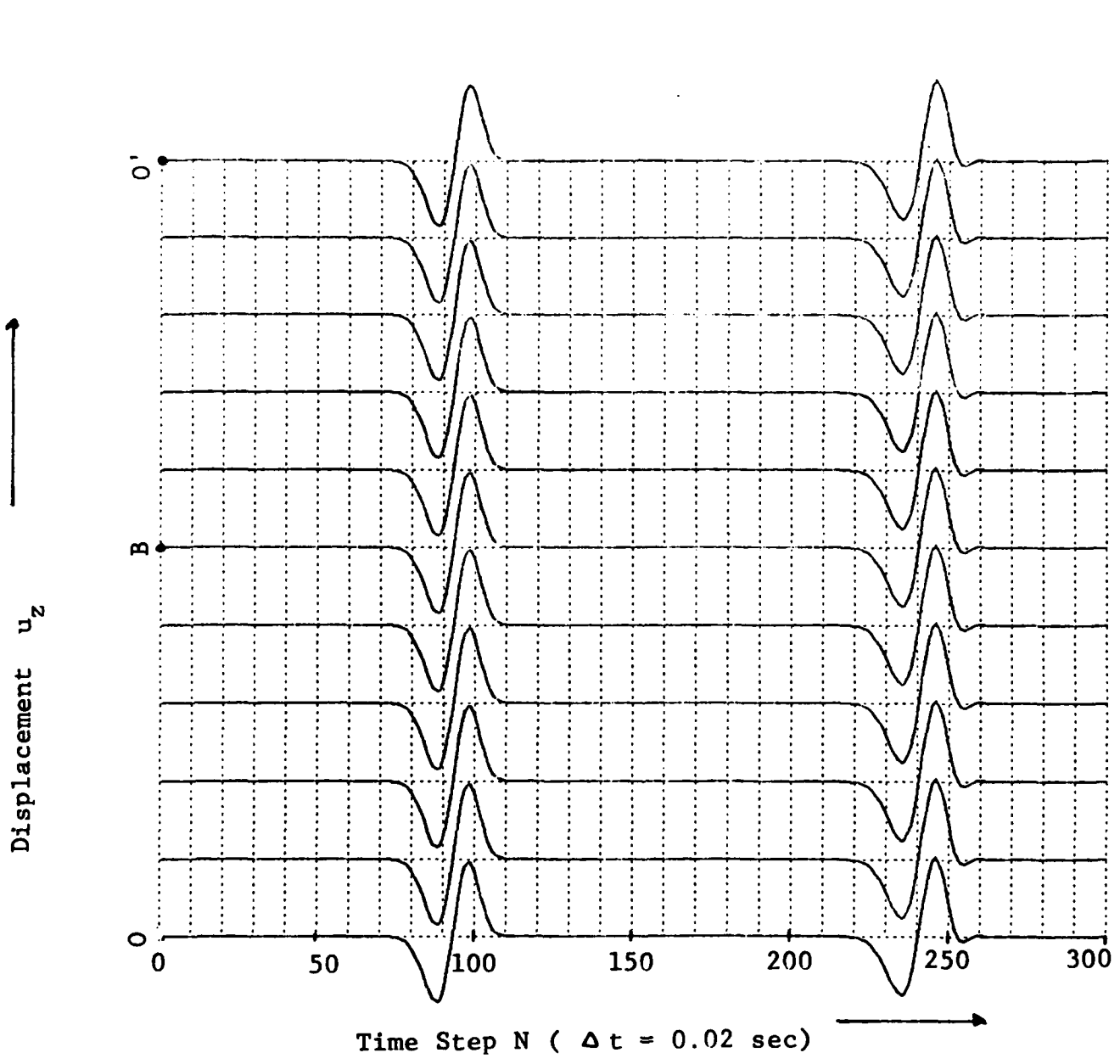

Figure 4. Synthetic Seismogram Along Free Surface OO' For Model 1.

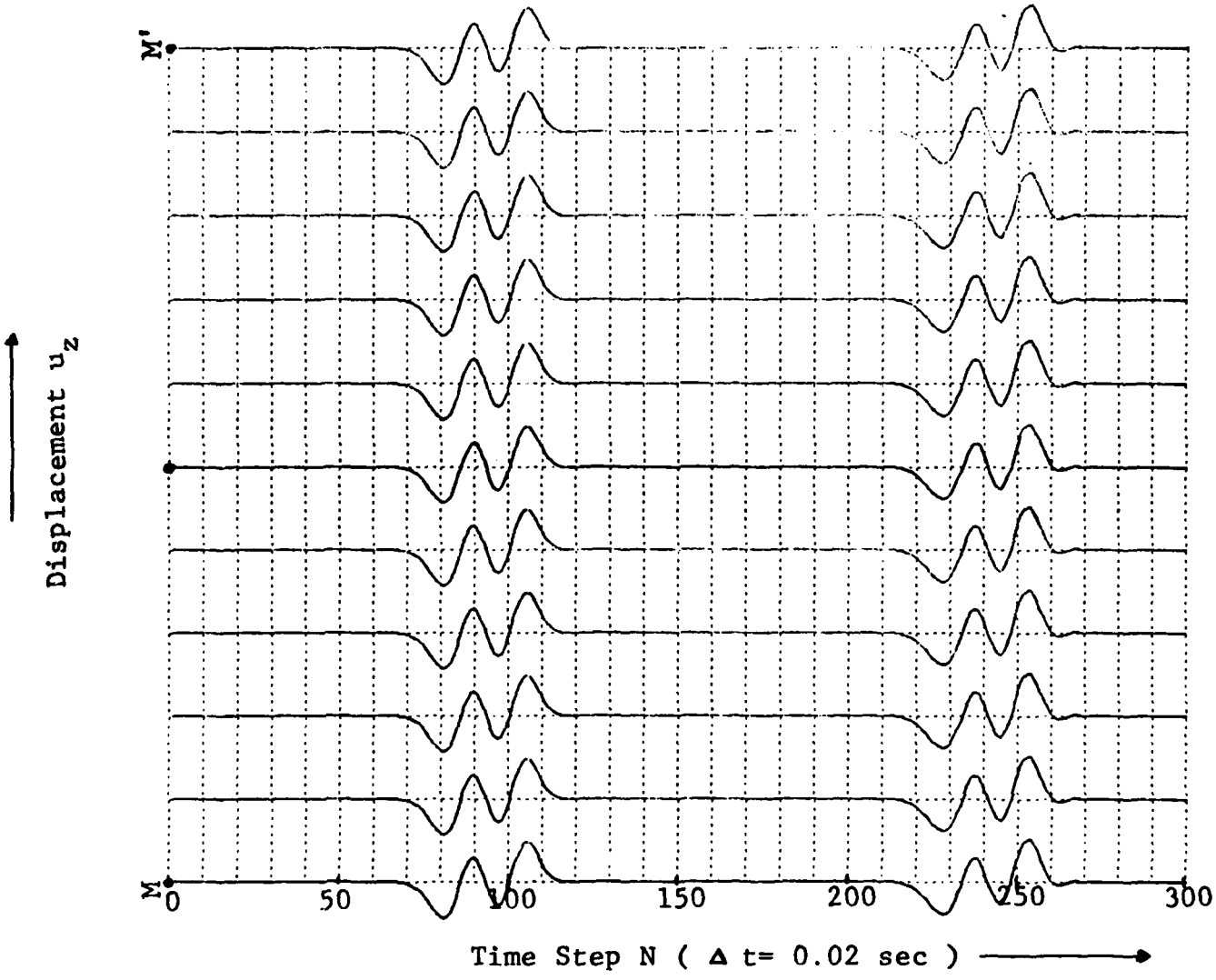

Figure 5. Synthetic Seismogram Along Horizontal Surface MM' For Model 1.

Model 2:

The exact same model as (a) above, except the upper left corner of 25 elements of medium 1 is replaced by medium 2. with a shear wave velocity v_{s2}= 1,750 m/sec, density ρ_2 = 2.4 gm/cm. The excitation function is identical to that in Model 1.

Figs. 7 and 8 show the results of the displacements u_z along the vertical planes OA and BC. The inclusion of medium 2 introduces a great deal of complexity of the waves. In Figs. 7 and 8, the direct waves and first reflection from the free surface 00' are still identifiable; however, t diffracted waves and multi-reflected waves in medium 2 giv he complex wave forms of the reflected waves at 00', with . re-sult that the reflected waves from AA' are distorted. As expected, the responses of displacements u_z along any horizontal surfaces are no longer idential as compared with those in Fig. 5. Figs. 9 and 10 are the synthetic seismograms along the horizontal surfaces NN' and MM'.

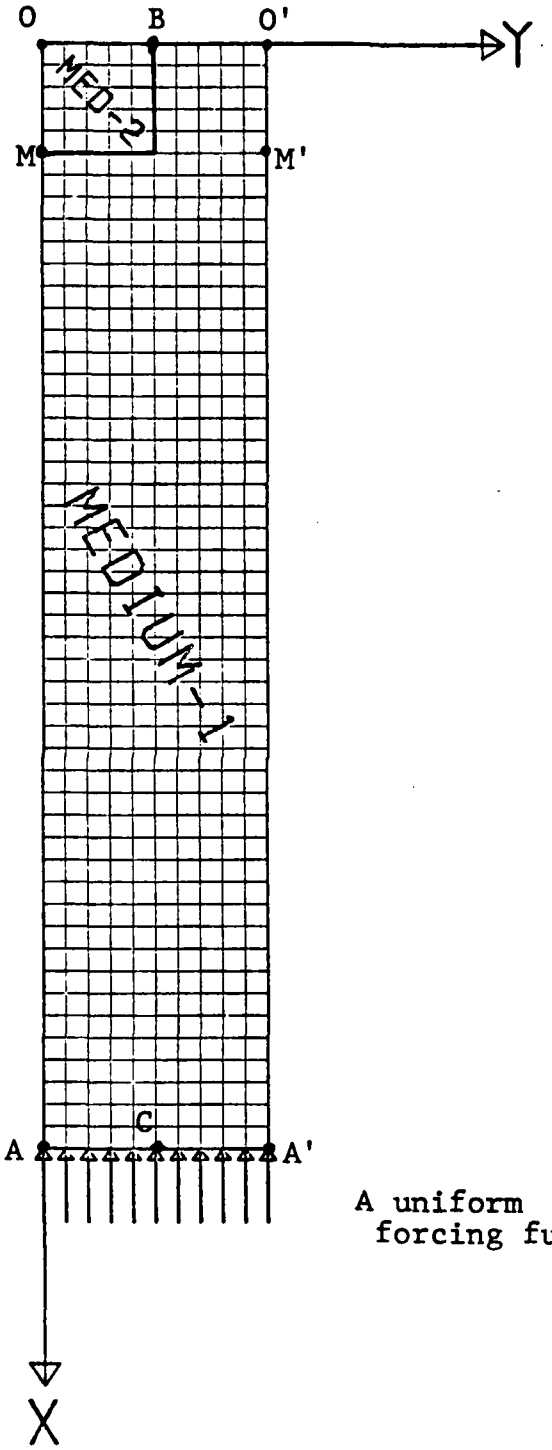

$\Delta x = \Delta y = 85$ m

$v_{s1} = 2{,}900$ m/sec

$\rho_1 = 2.67$ gm/cm^3

$v_{s2} = 1{,}750$ m/sec

$\rho_2 = 2.40$ gm/cu^3

A uniform SH wave forcing function

Figure 6. Finite Element Model 2.

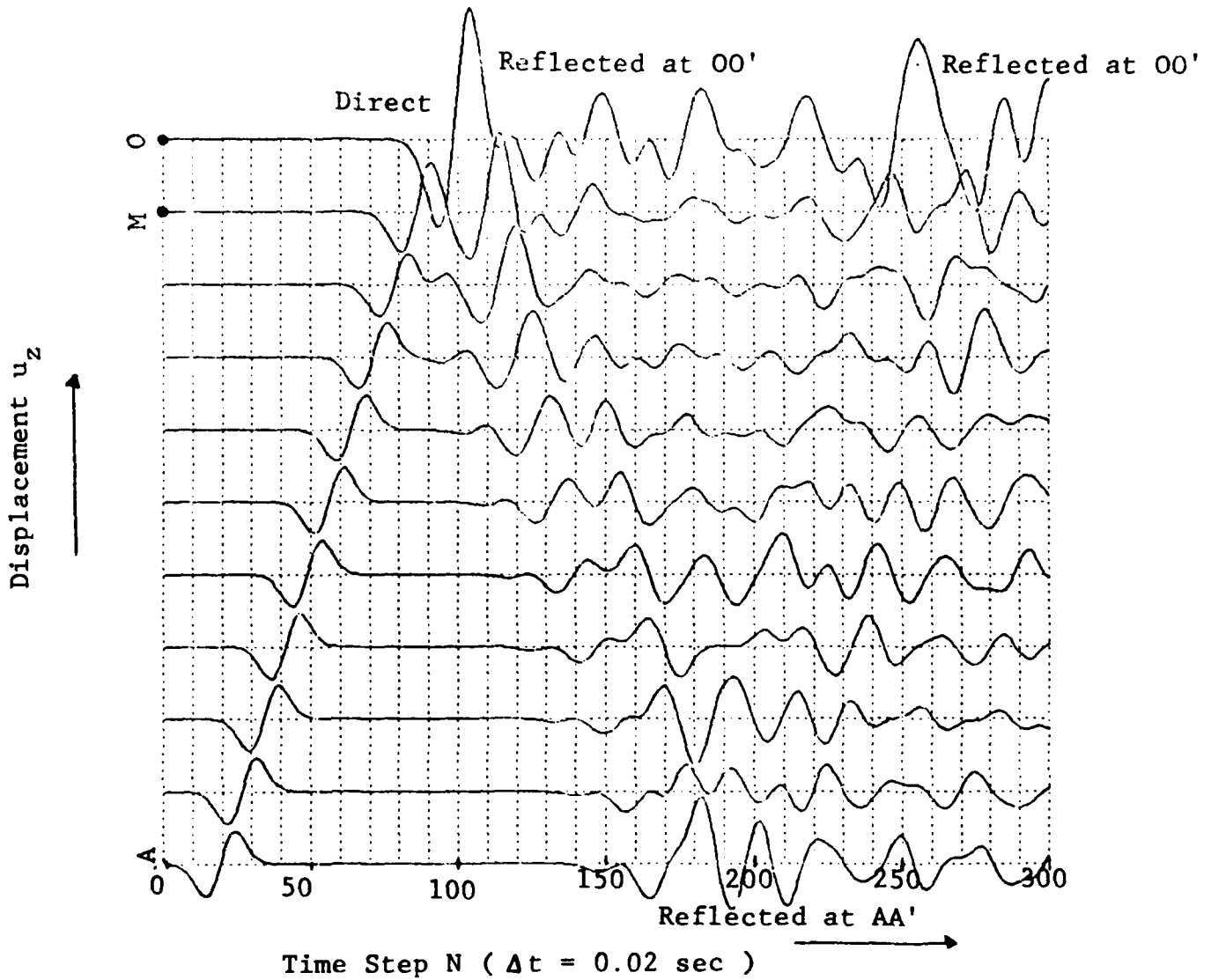

Figure 7. Synthetic Seismogram Along Vertical Plane OA for Model 2.

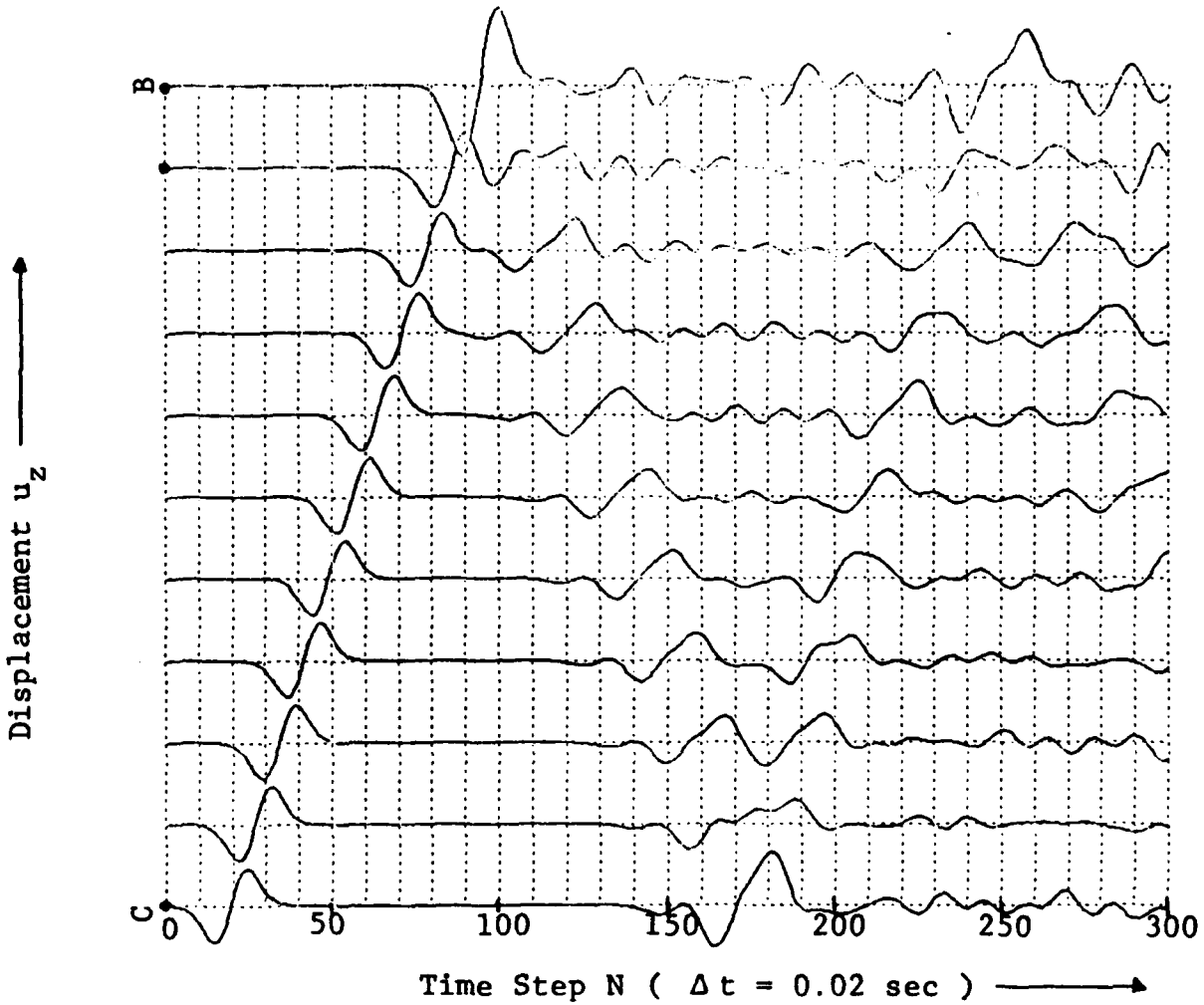

Figure 8. Synthetic Seismogram Along Vertical Plane BC For Model 2.

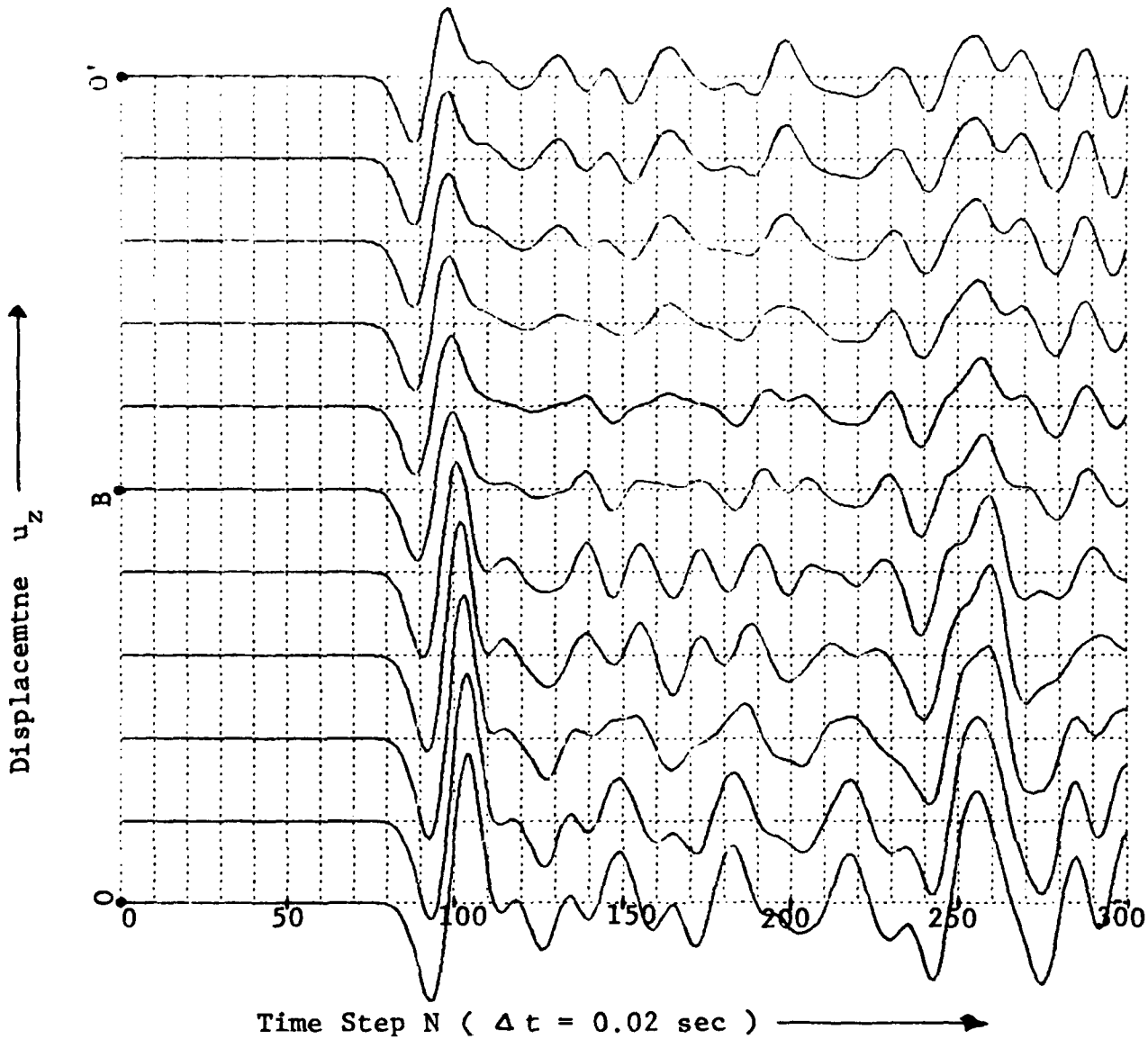

Figure 9. Synthetic Seismogram Along Free Surface OO' For Model 2.

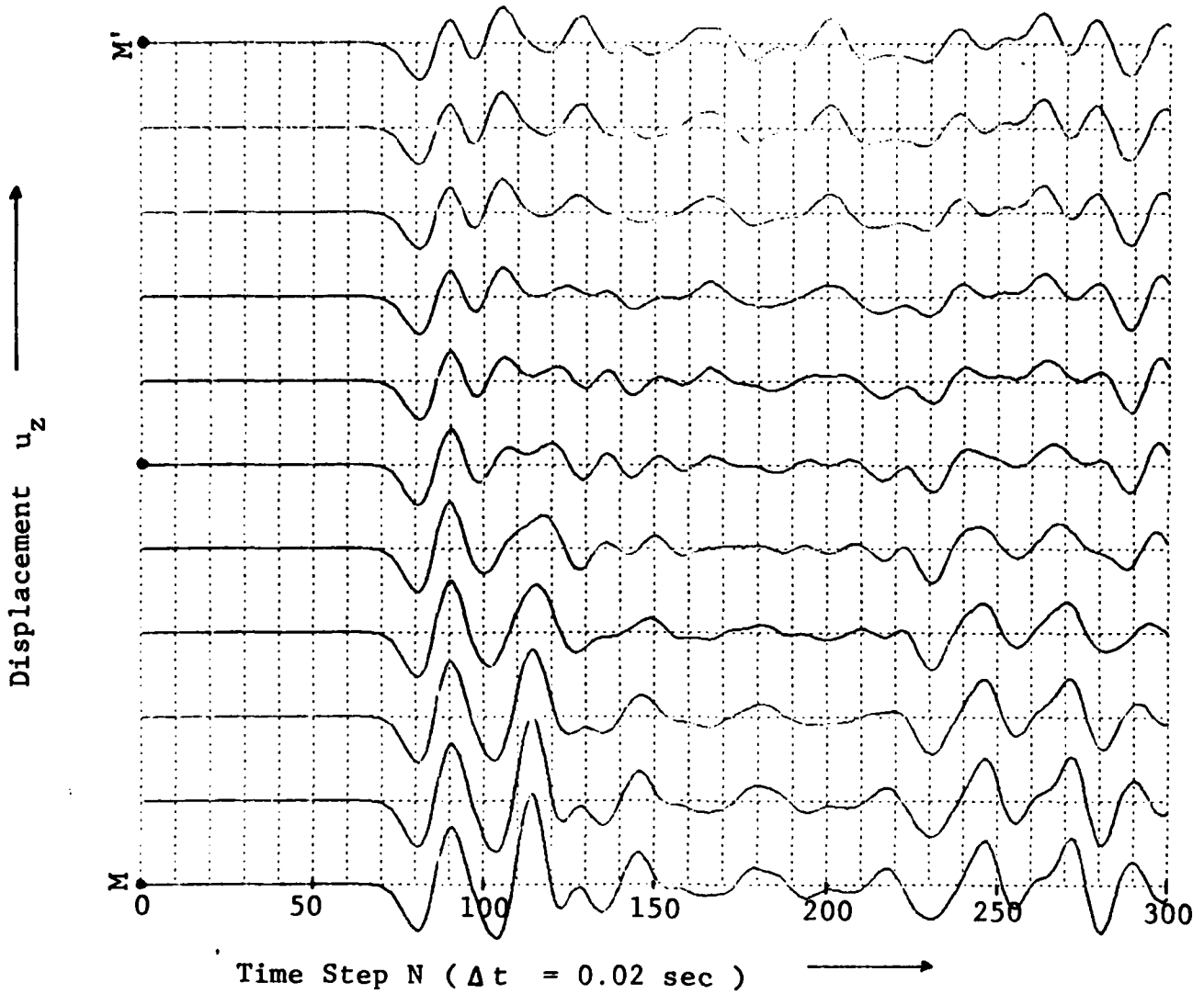

Figure 10. Synthetic Seismogram Along Horizontal Surface MM' For Model 2.

Model 3:

In this section, two partial basins are modeled. The same homogeneous material as Model 1 above, but with a different geometry as shown in Figs. 11 (Model 3-a) and 12 (Model 3-b). In Fig. 11, an SH wave line source is excited at Point S on the free surface of the deeper basin DC, while the receivers are located on the free surface of the shallower basin in the region BC. For Model 3-b (in Fig. 12), an SH source is located in the shallower basin, while the receivers are in the deeper basins. Again, the forcing function is the first derivative of a Gaussian function with its center frequency $f_c \sim 2.5$ Hz. The calculated displacements u_z for Models 3-a and 3-b obtained along ABC in both models are shown in Figs. 13 and 14, respectively. In Figs. 13 and 14, as expected, at the corner B, waves change their magnitude and phase. It is obvious that the reflection from plane DB causes drastic changes in phase and amplitude in the case of Model 3-b. From the distortion of these waves due to the corner, as the position ABS' is in the Shadow zone shown in Fig. 13, we may conclude that since the arrivals at the position ABS' are the diffracted waves at O the effect of diffraction due to the corner is small in comparison with the direct waves as received at the position ABS' in Model 3b (Fig 12). Figs. 13 and 14 demonstrate the reciprocity of source and receiver by the responses observed at ponit S'.

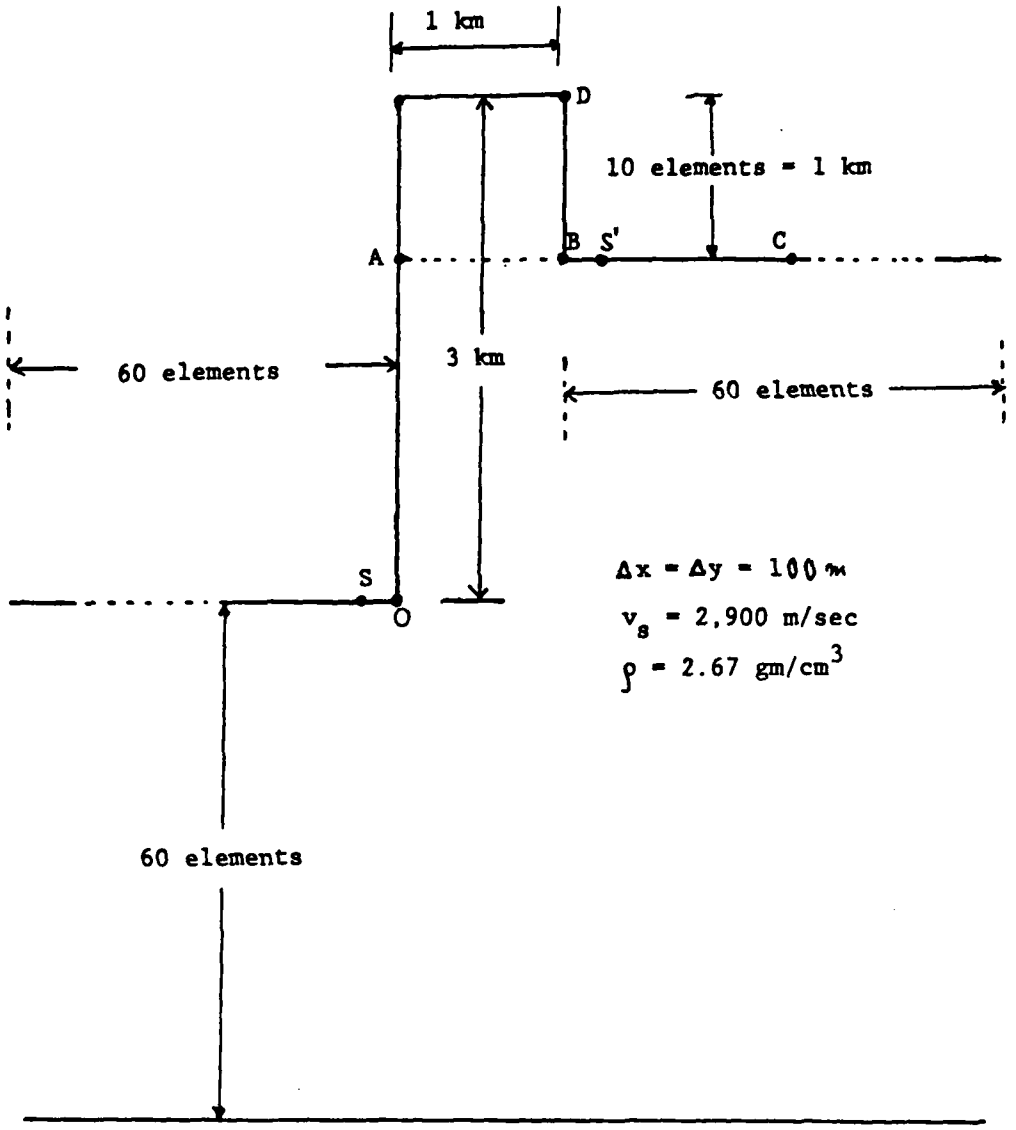

Figure 11. Preliminary Basin Model 3-a.

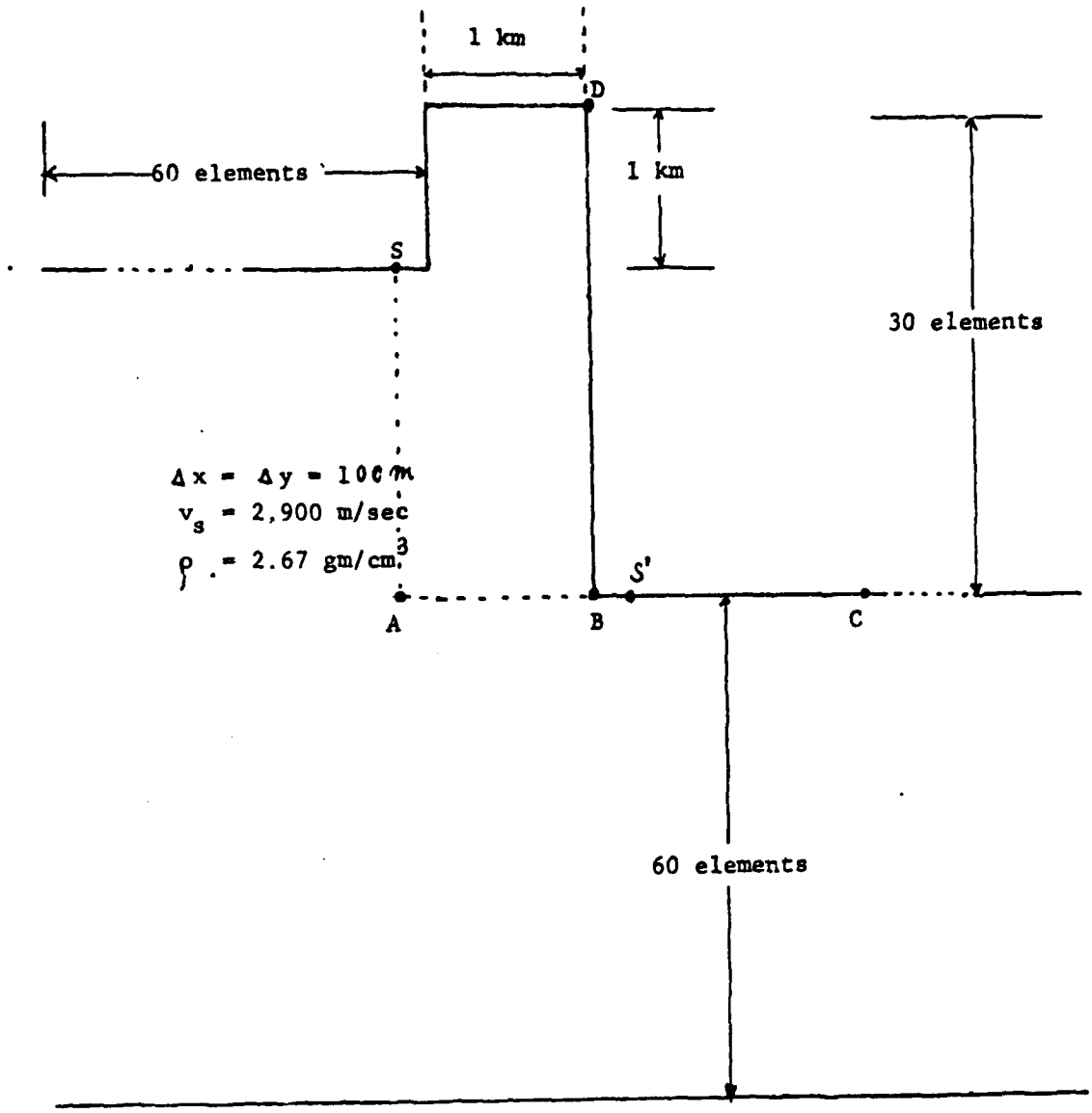

Figure 12. Preliminary Basin Model 3-b.

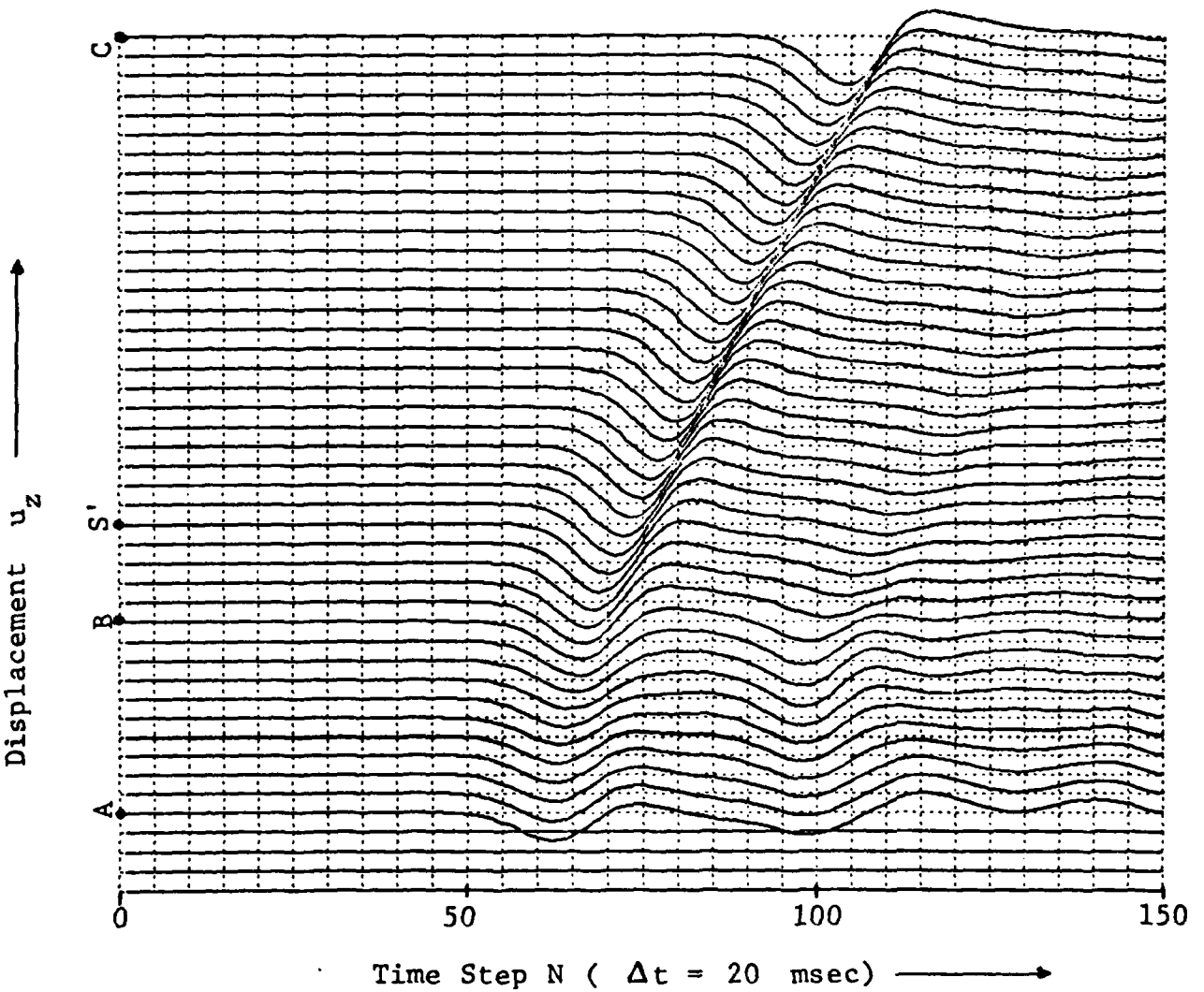

Figure 13. Synthetic Seismogram Along ABC of Model 3-a.

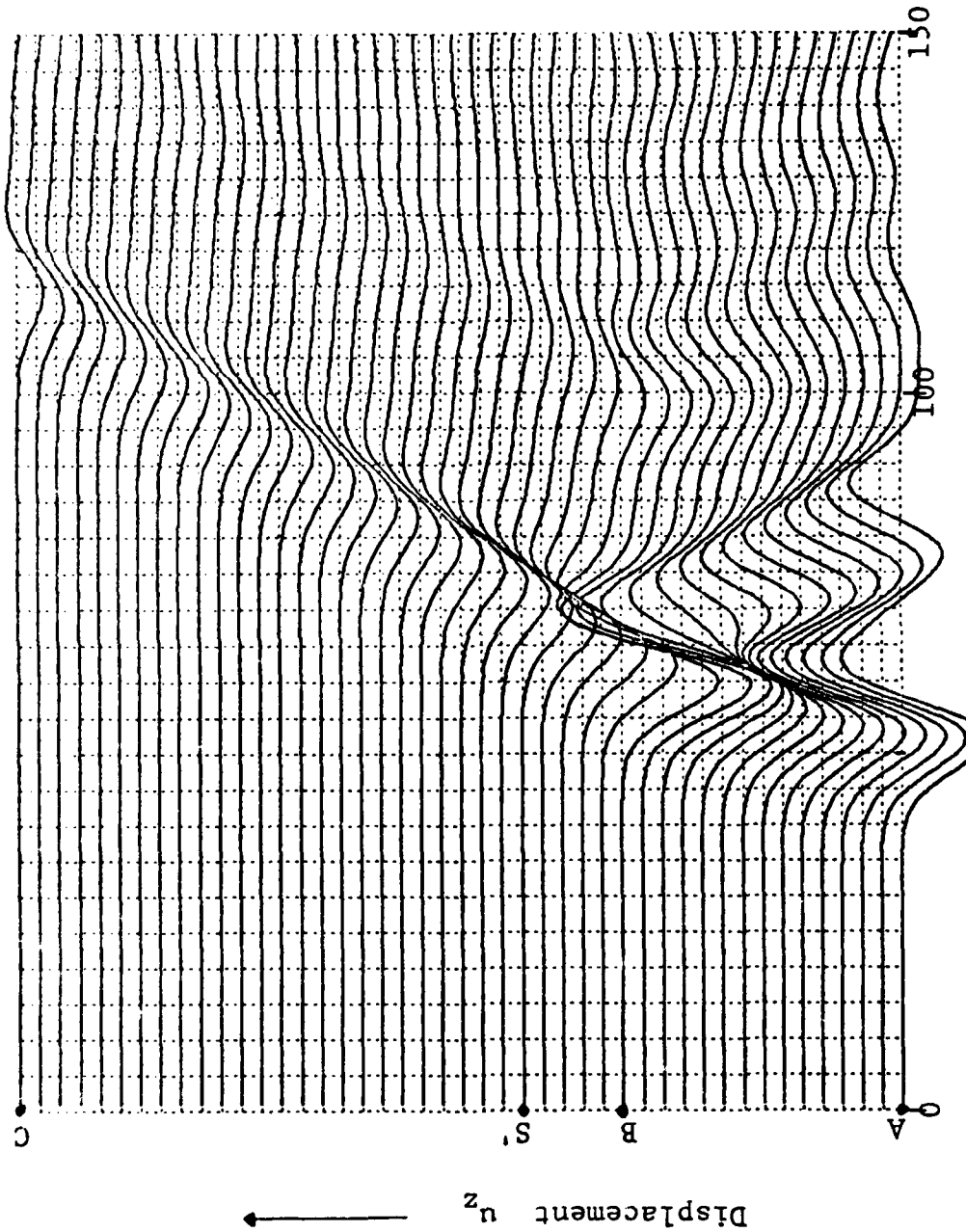

Figure 14. Synthetic Seismogram Along ABC of Model 3-b.

(b) Comparison of Numerical Results With Analytical Results for SH Waves

In order to assure the accuracy of the results of finite element modeling, we have used a larger finite element model with an internal source compared with the known analytic solutions. Fig. 15 shows the finite element model for an SH source located at center and recorded at locations 1, 2, 3, and 4, with a shear velocity of v_s = 2,900 m/sec, density ρ = 2.67 gm/cm^3, $\Delta x = \Delta y$ = 58 m, with 10,000 quadrilateral elements. The results of relative displacement at all locations agree with those of analytic solutions within about 2% deviation as shown in Fig. 16. The analytical solutions are obtained by convolving the external forcing function with the Green's function of the problem.

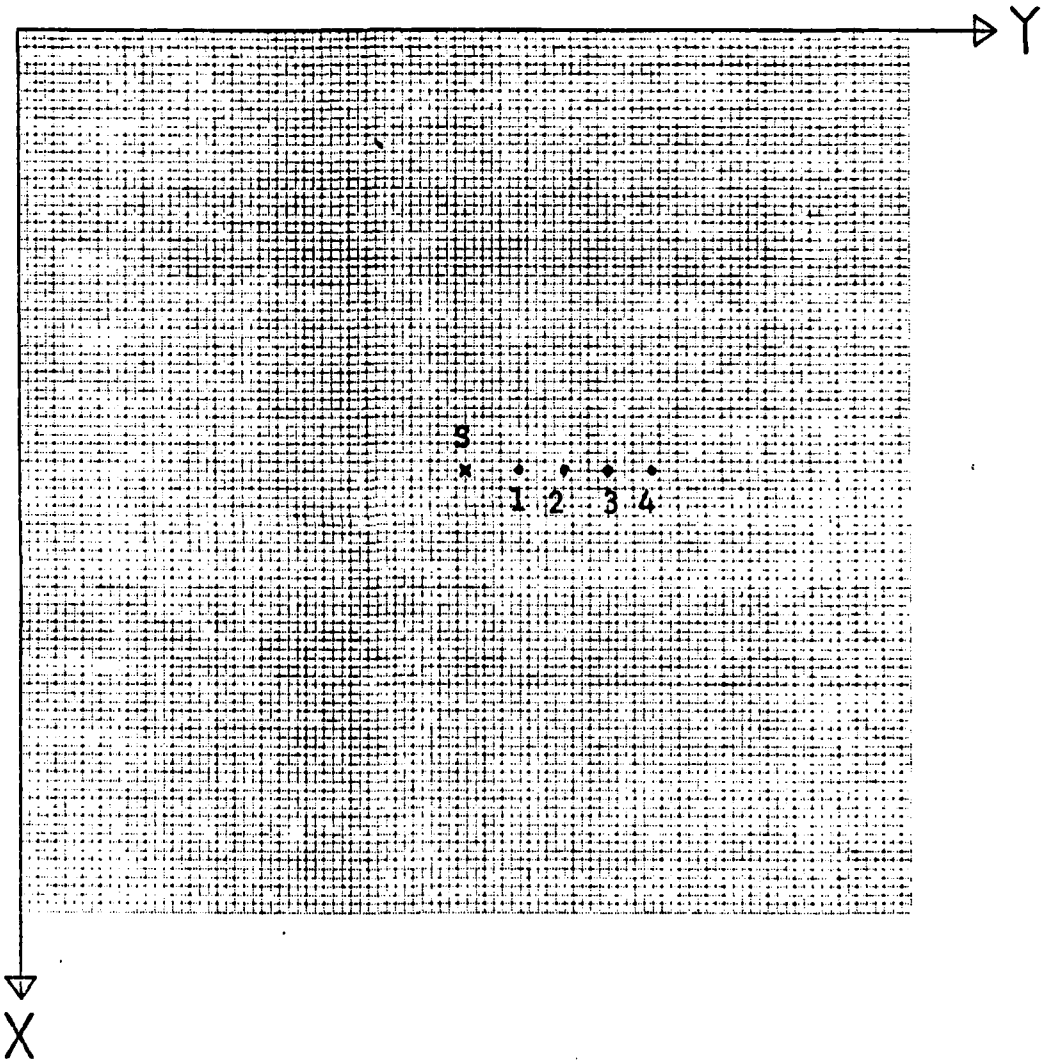

Figure 15. A Larger Finite Element Model to Compare Numerical Results With Analytical Results.

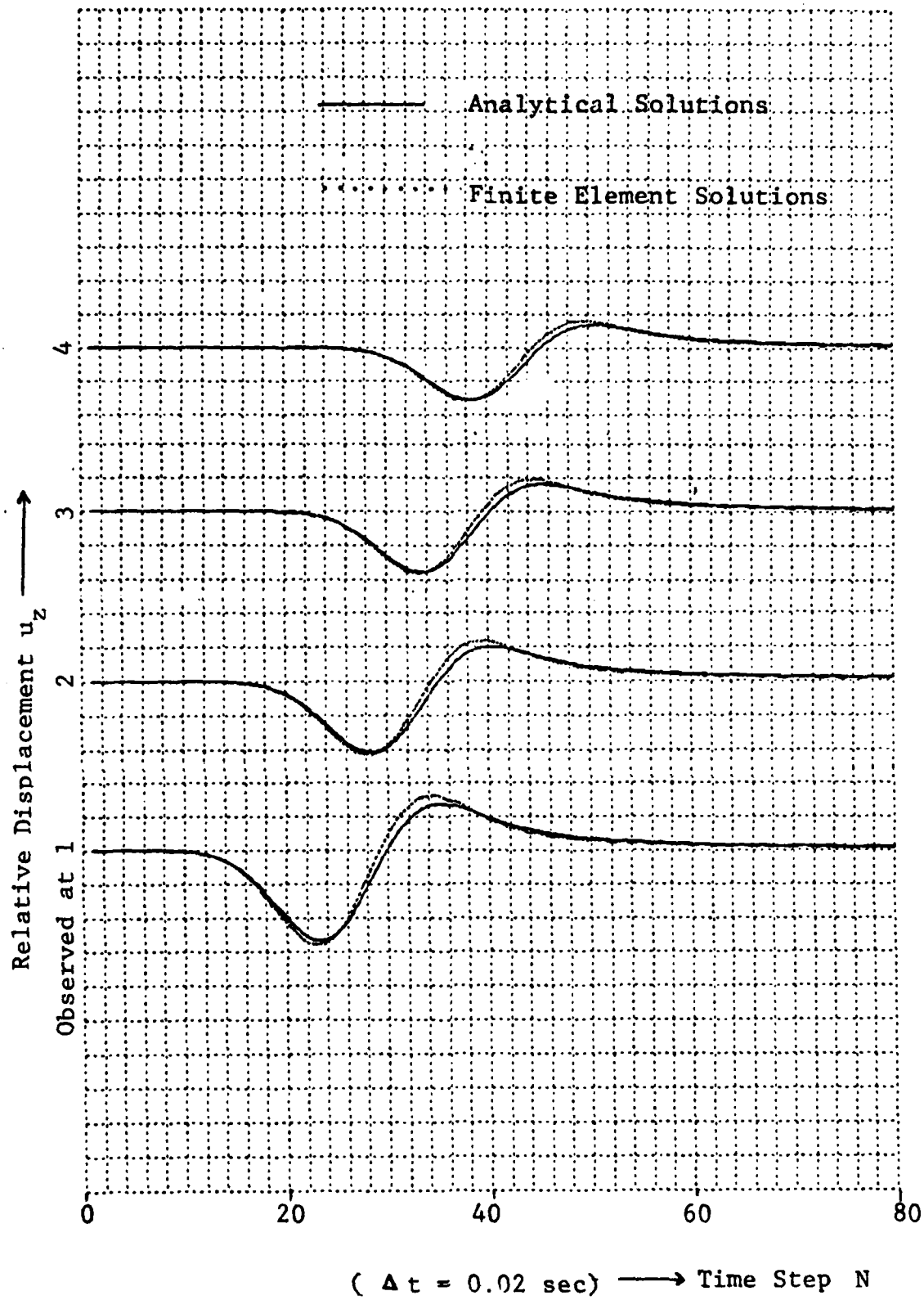

Figure 16. Comparison of the Finite Element and the Analytical Solutions. (Observed at Points 1,2,3,4).

(c) Two Adjacent Alluvial Basins for Elastic Waves (P and S Waves)

The basin is filled with 3 km sediments (v_{p2} = 3,500 m/sec, v_{s2} = 1,905 m/sec, ρ_2 = 2.5 gm/cm^3), which are overlain by a surface low velocity layer (v_{p1} = 2,200 m/sec, v_{s1} = 1,180 m/sec, ρ_1 = 2.3 gm/cm^3). The bedrock of the basement assumes v_{p3} = 5,500 m/sec, v_{s3} = 3,175 m/sec, ρ_3 = 2.7 gm/cm^3. The basin B is 15 km in width and filled with exactly the same materials as basin A. The basement is bounded by a rigid halfspace. The total length of the two alluvial basin models is 50 km. The thickness of the model is 7 km. Fig. 17 shows the complete finite element model.

A vertical force source load is located in a smaller basin (Basin A in Fig. 17a) with a width of 10 km. The source forcing function F_o used in the finite element calculation is that of the first derivative with respect to time of a Gaussian function as shown in Fig. 18. In order to obtain a stable and valid solution, we have to choose a time step Δt which satisfies the Courant-Friedrickson-Lewy (CFL) condition and an element dimension Δs to be small enough so that one wavelength can be approximately simulated by 10 Δs. In doing so, the width of the forcing function N Δt should be greater than a factor of about $(8.3\ v_{max}\ \Delta t)/v_{min}$, where v_{max} and v_{min} are the largest and the smallest velocities in the whole finite element model.

For the alluvial basin finite element model, we use a source function with a pulse width 160 Δt (N=40). A total of approximately 70,000 elements is required for such a model, if the center frequency of the forcing function is about 1 Hz, with a total number of equations of motion of 140,000. Figs. 19a to 20b are the preliminary results obtained from the model. Figs. 19a and 19b are the synthetic seismograms of vertical and horizontal displacements, which are normalized to the displacement of the forcing function at the loading position, at various nodal points along the surface SO_1 (see Fig. 17b). Figs. 20a and 20b are the same synthetic seismograms along nodal points on BO_2 with a 10 times larger scale than those in Figs. 19a and 19b. As expected, at the corners B and C drastic changes in magnitude and phase can be clearly observed.

Because of the complexity of the model, further study is in progress.

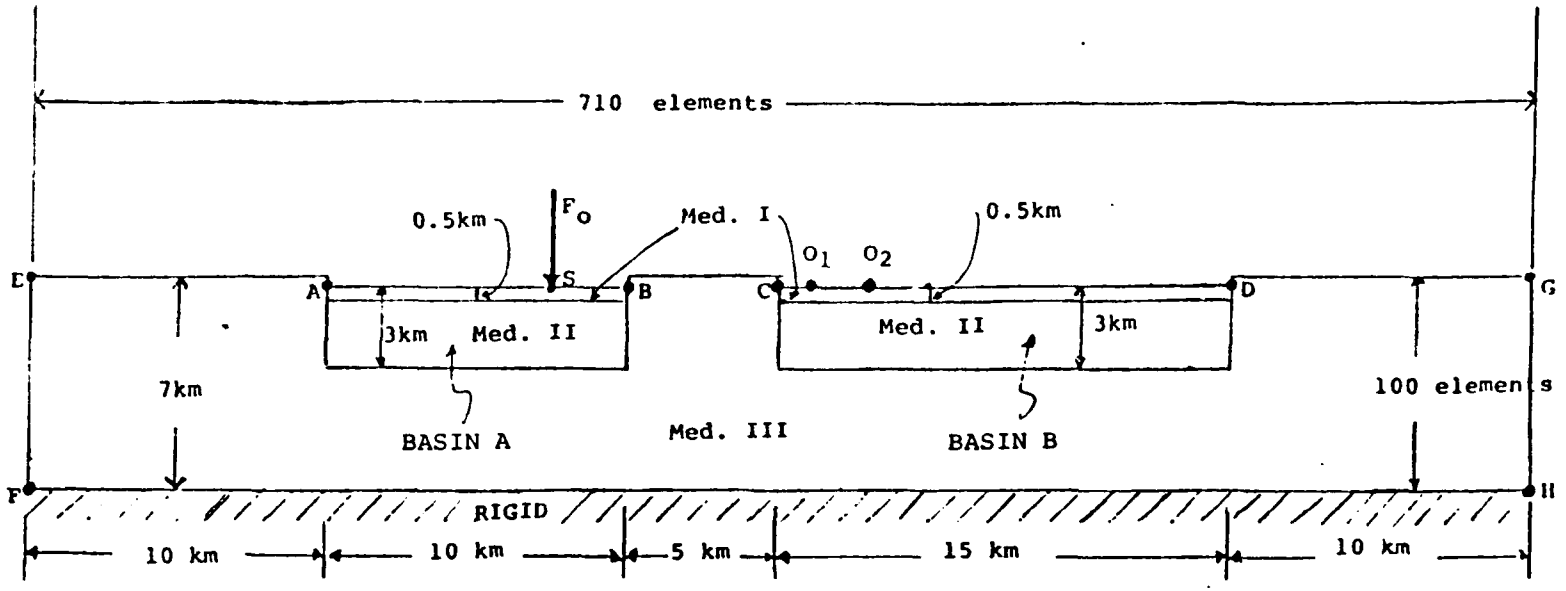

ρ_1 = 2.3 gm/cm^3 , V_{p1}=2,200 m/sec , V_{s1} = 1,180 m/sec,

ρ_2 = 2.5 gm/cm^3 , V_{p2}= 3,300 m/sec , V_{s2} = 1,905 m/sec,

ρ_3 = 2.7 gm/cm^3 , V_{p3}= 5,500 m/sec , V_{s3} = 3,175 m/sec.

Figure 17. Finite Element Model for the Problem of Ground Response in Two Basins Due to Seismic Disturbances.

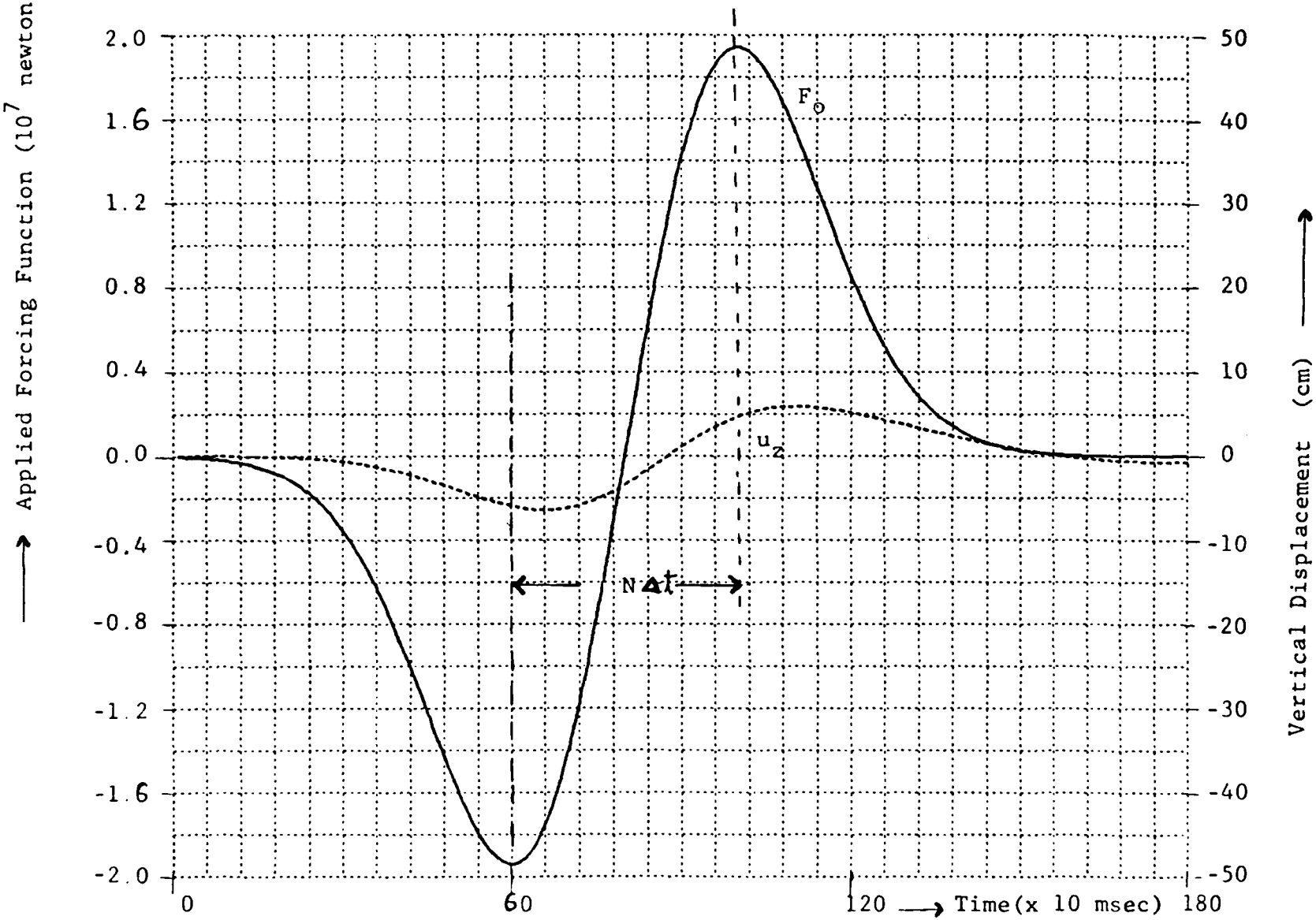

Figure 18. ——— Distribution of Time Dependant Forcing Function.

----- Distribution of Vertical Displacement at the Loading Position.

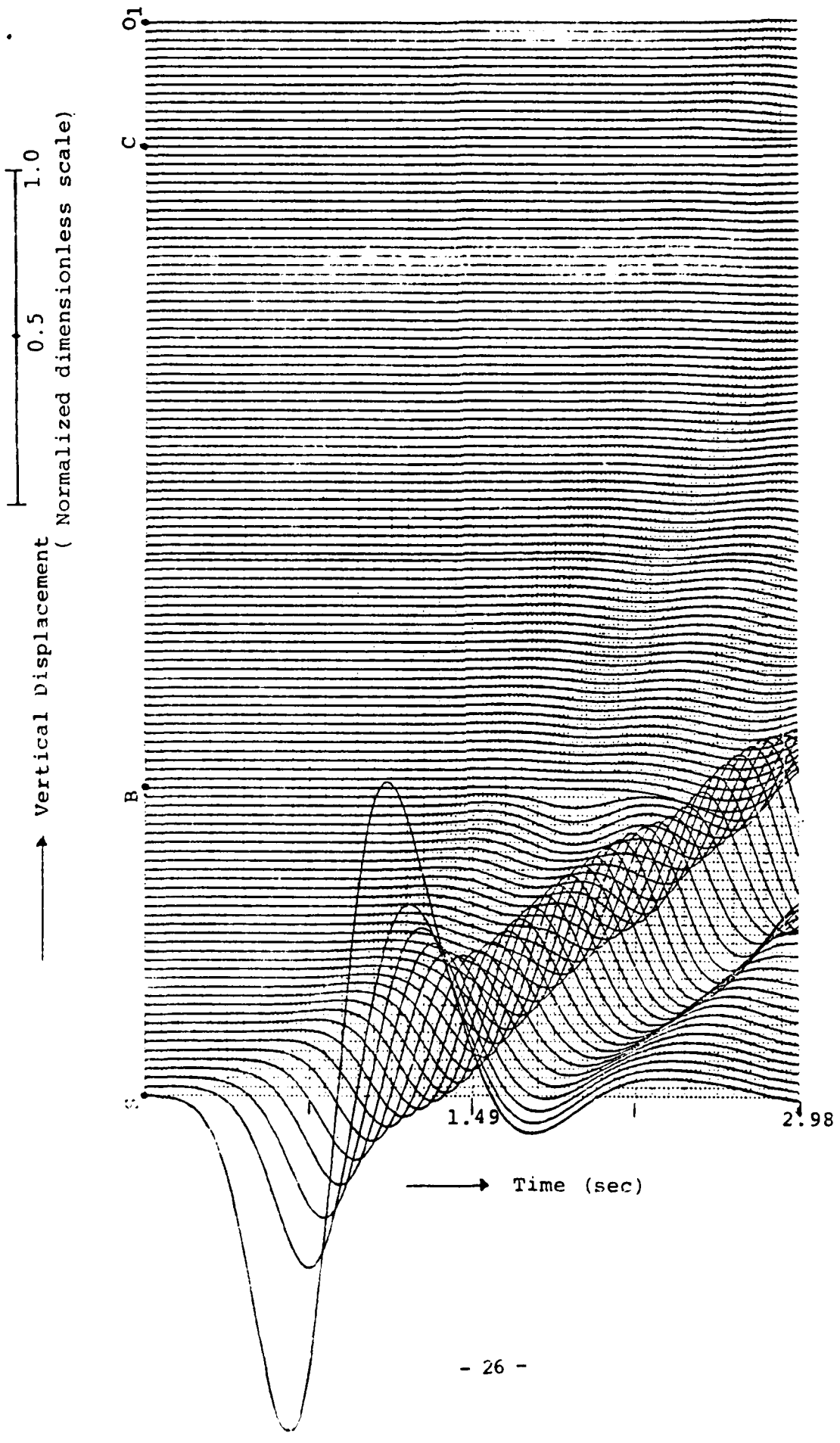

Figure 19a. Vertical Displacement Along Surface SO_1 .

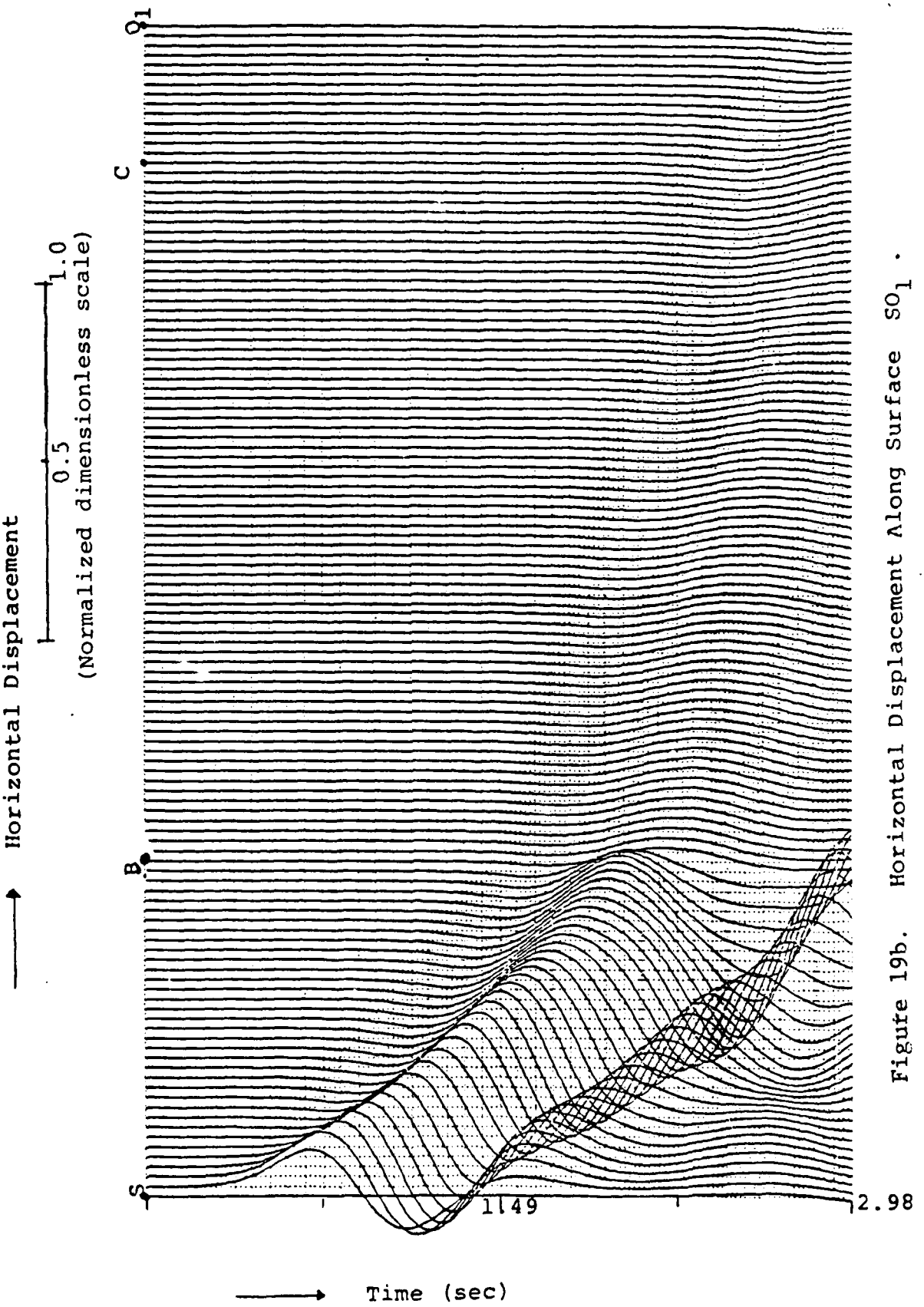

Figure 19b. Horizontal Displacement Along Surface SO_1.

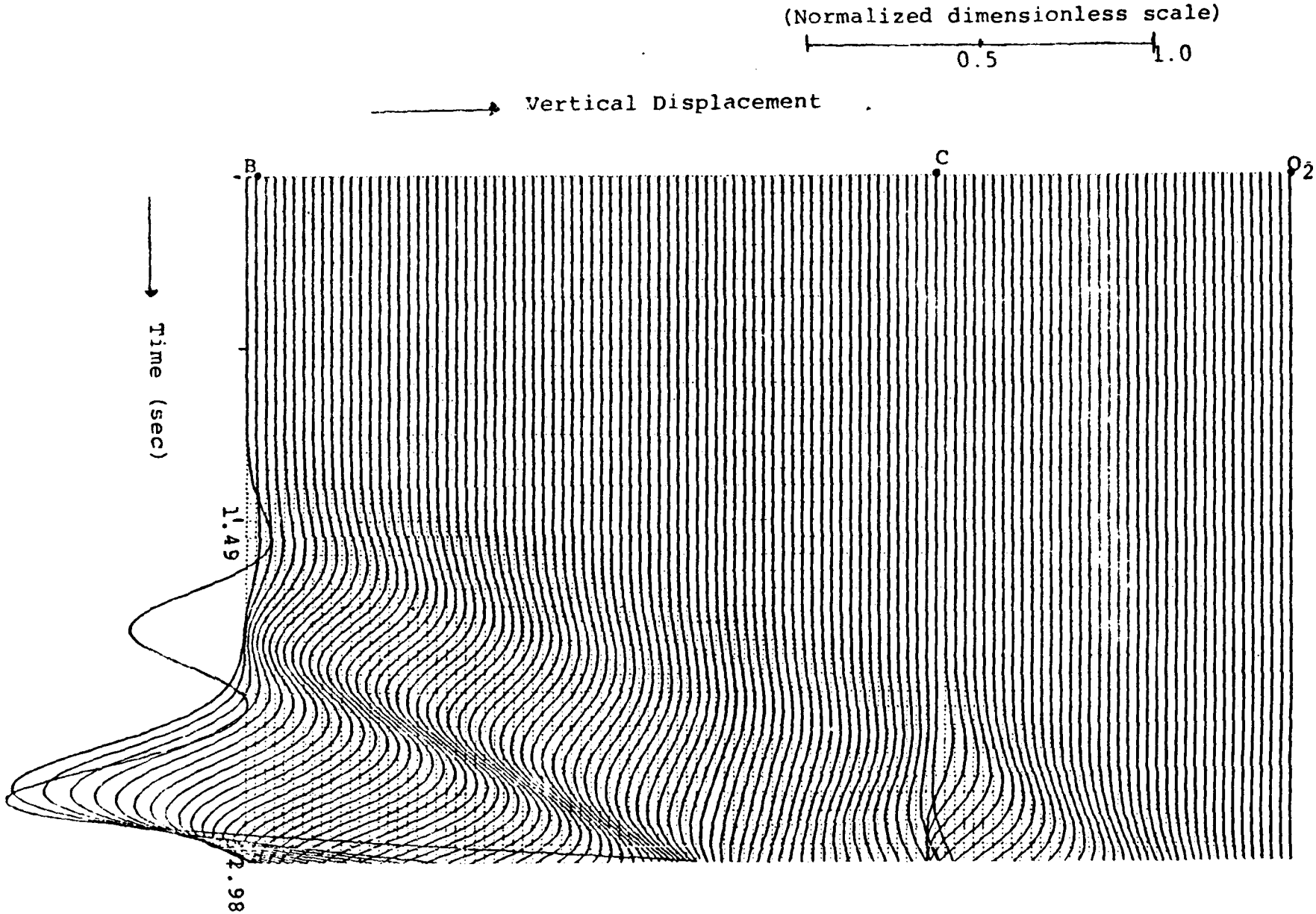

Figure 20a. Vertical Displacement Along Surface BO_2.

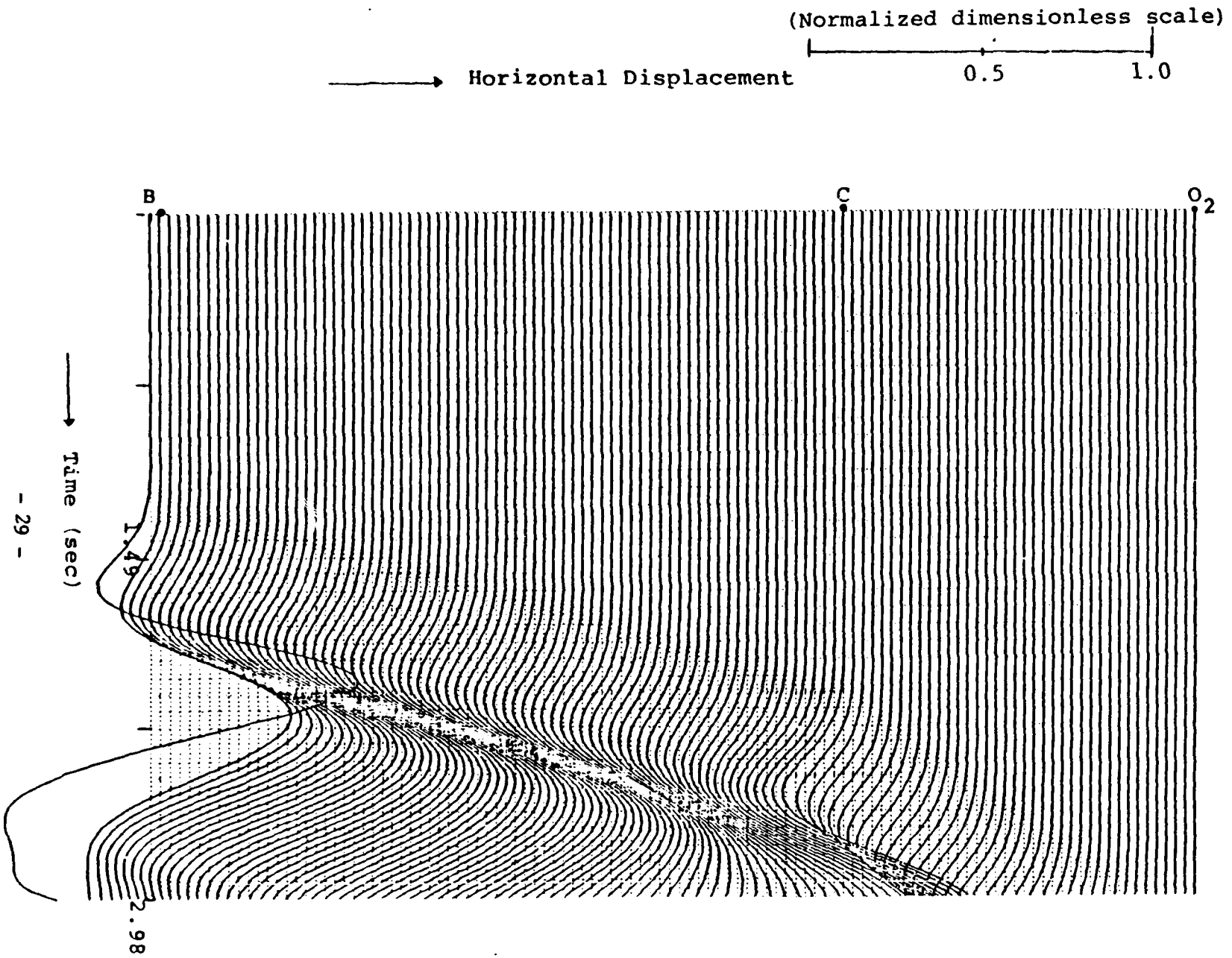

Figure 20b. Horizontal Displacement Along Surface BO_2 .

II. Modification and Improvement of the Two Dimensional Finite Element Computer Codes

(a) Non-Reflecting Boundaries

The truncation of finite element models generates undesirable reflections from the truncated boundaries. Numerical analysis techniques which attempt to eliminate these undesirable reflections generally involve either viscous boundary or superposition boundaries to simulate the transparent boundaries. In the frequency domain finite element computer modeling, Lysmer and Kuhlemeyer (1969) and White et al. (1977) propose using viscous dashpots to damp out most of the reflections. However, within the framework of the time domain solutions, the viscous dashpot technique is good for elastic body waves but not for surface waves. Also, the damping is frequency and incident angle dependent. Smith (1973) proposes a superposition method by adding two separate solutions, one with a Dirichlet and one with a Neumann boundary condition, to eliminate the artificial reflections. Although Smith's formulation is independent of both frequency and incidence angle, it requires 2^n complete dynamic solutions if there are n reflecting surfaces. This method also fails when a given wave is reflected at the same boundary more than once.

After considerable effort, we have succeeded in refining Smith's superposition method, which is referred here as modified Smith superposition method for non-reflecting boundaries, summarized as follows:

(1) For one degree of freedom problems (acoustic or SH waves).

(i) Calculate the solution for Neumann's problem for each nodal point of the whole structure.

(ii) Divide the solution obtained from Neumann's problem by 2 at the boundaries to obtain the expected solutions at the boundaries of each time step.

(iii) Use these expected values at the boundaries as feedback boundary conditions to calculate the expected responses of the interior nodal points for the same time step.

(2) For two degree of freedom problems (two-dimensional elastic waves).

(i) Calculate the solution for the mix boundary conditions 1, i.e., normal displacement and tangential stress at the boundary are zero.

(ii) Calculate the solution for the mix boundary conditions 2, i.e., tangential displacement and normal stress at boundary are zero.

(iii) Divide the tangential displacement at the boundary obtained from (i), and the normal displacement at the boundary obtained from (ii) to obtain the recovered displacement components at the boundaries at each time step.

(iv) Use these expected values of displacements at the boundaries as feedback boundary conditions to calculate the expected responses of the interior nodal points for the same time step.

The proposed approach avoids the need for 2^n complete solutions if there are n reflecting surfaces. However, this method still fails when a given wave is reflected at the same boundary more than once.

The following are two finite element models to demonstrate the cancellation of reflections.

Example 1:

An infinite long elastic plate, bounded by an upper

free surface and a lower rigid surface, with wave velocities v_p = 2,000 m/sec, v_s = 1,155 m/sec, density ρ = 2.4 gm/cm^3 (Fig. 21a). Use of symmetry is made by letting the horizontal displacement along z-axis be zero, to reduce the size of the problem (Fig. 21b). We use an internal forcing function F_o with a time step = 5.0 x 10^{-3} sec. The observation points are located at A and B. The grid sizes are Δx = 16 m and Δz = 15 m. First, construct a model of sufficiently large size (150 x 46 elements), to obtain the required solution before the arrivals of the reflection from the side boundaries (MM' and NN' in Fig. 21a). Then construct a model of smaller size (20 x 46 elements) with the application of the above described non-reflecting boundary conditions along BB' to simulate an infinite medium along x-direction. Figs. 22a and 22b give the comparison of the displacement components between two different kinds of solutions observed at point B. The dotted curves are the expected results, the solid curves are the averaging values obtained with free and rigid boundary conditions on BB'. The deviation between the two different kinds of solutions starts at the twenty-first time step numerically. Figs. 22a and 22b show the comparison of the expected results and the non-reflecting boundary solutions based on the modified Smith superposition method observed at the same boundary point B. Exact cancellation has been effectively carried out until the boundary BB' becomes the second-time reflecting boundary for a given ray. Figs. 23a and 23b are the comparison of the two kinds of solutions observed at point A; the deviation would start at the thirty-first time step without applying the non-reflecting boundary contions.

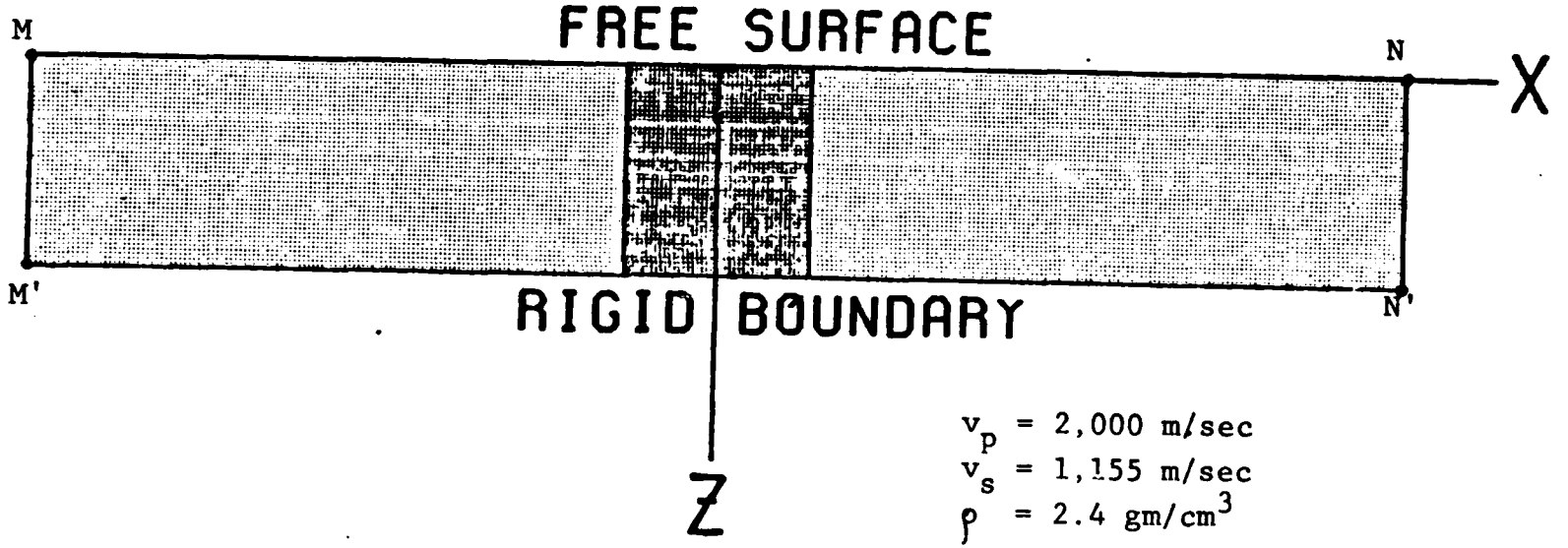

FINITE ELEMENT MODEL I

Figure 21a. Finite Element Model for an Infinite Elastic Plate.

(Dark Region is the simulated infinite plate with the use of the non-reflecting boundaries.)

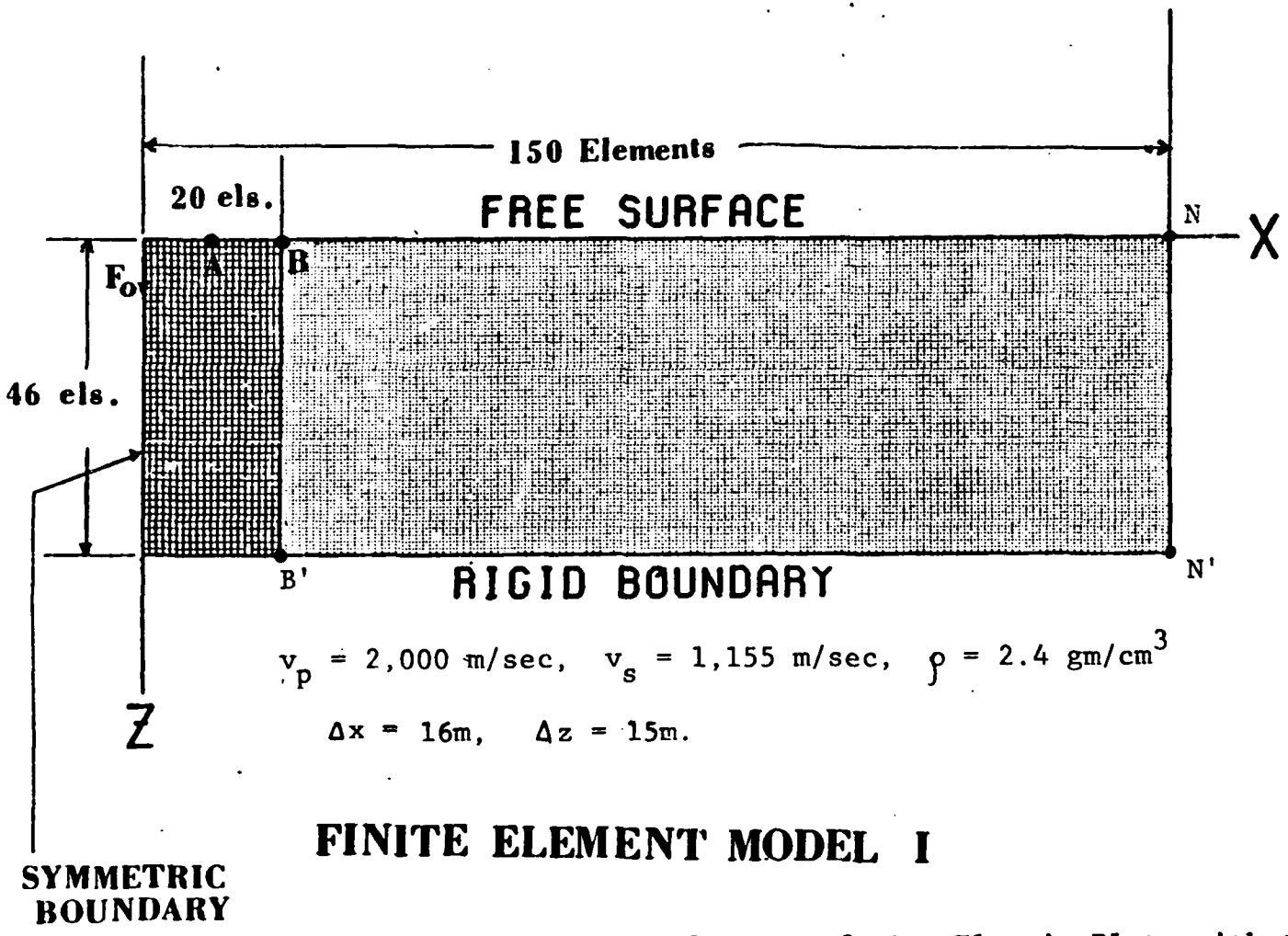

FINITE ELEMENT MODEL I

Figure 21b. Finite Element Mesh for an Infinite Elastic Plate with the Use of the Symmetric Boundary Conditions.

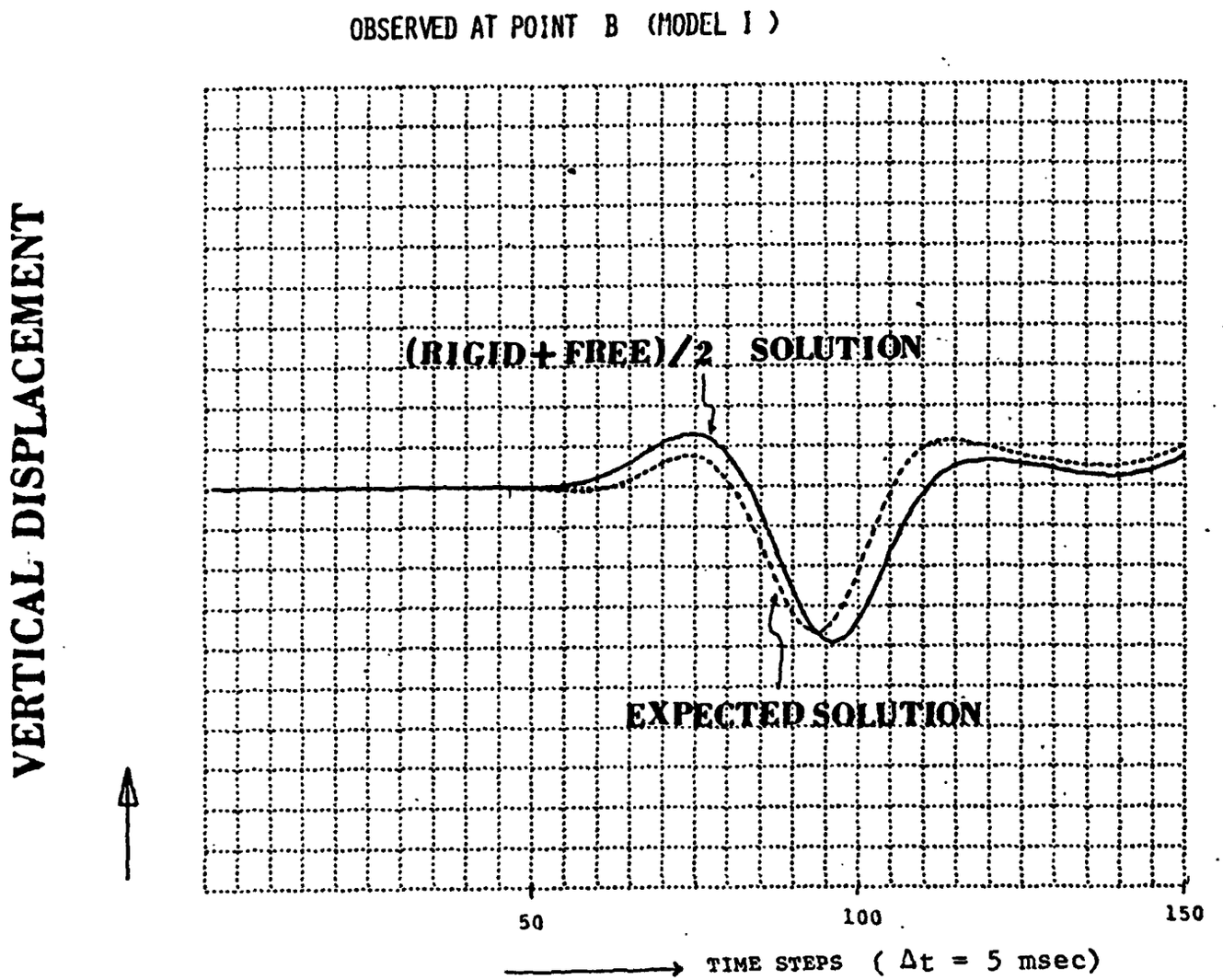

Figure 22a. Comparison of Vertical Displacements.

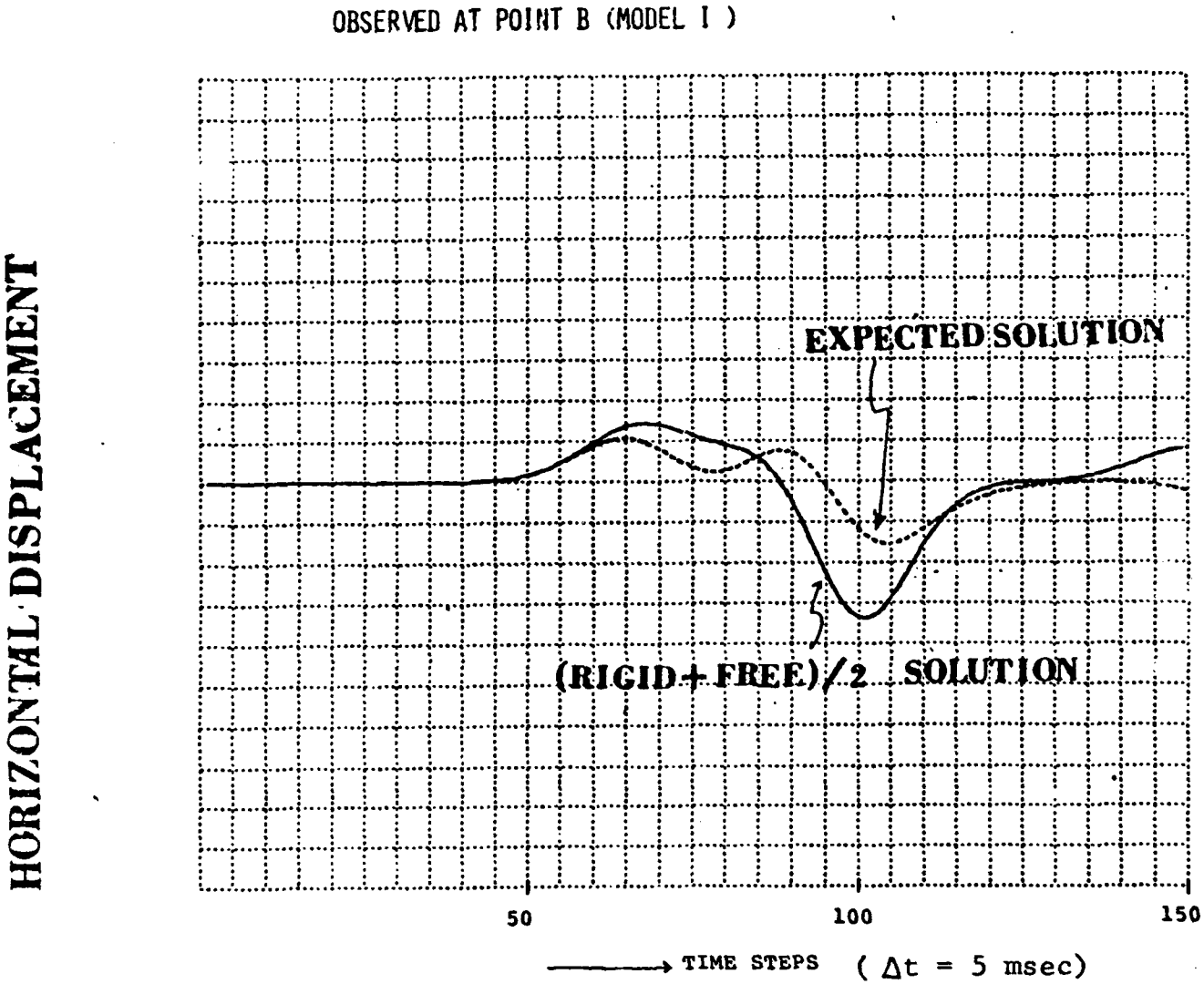

Figure 22b. Comparison of Horzontal Displacements.

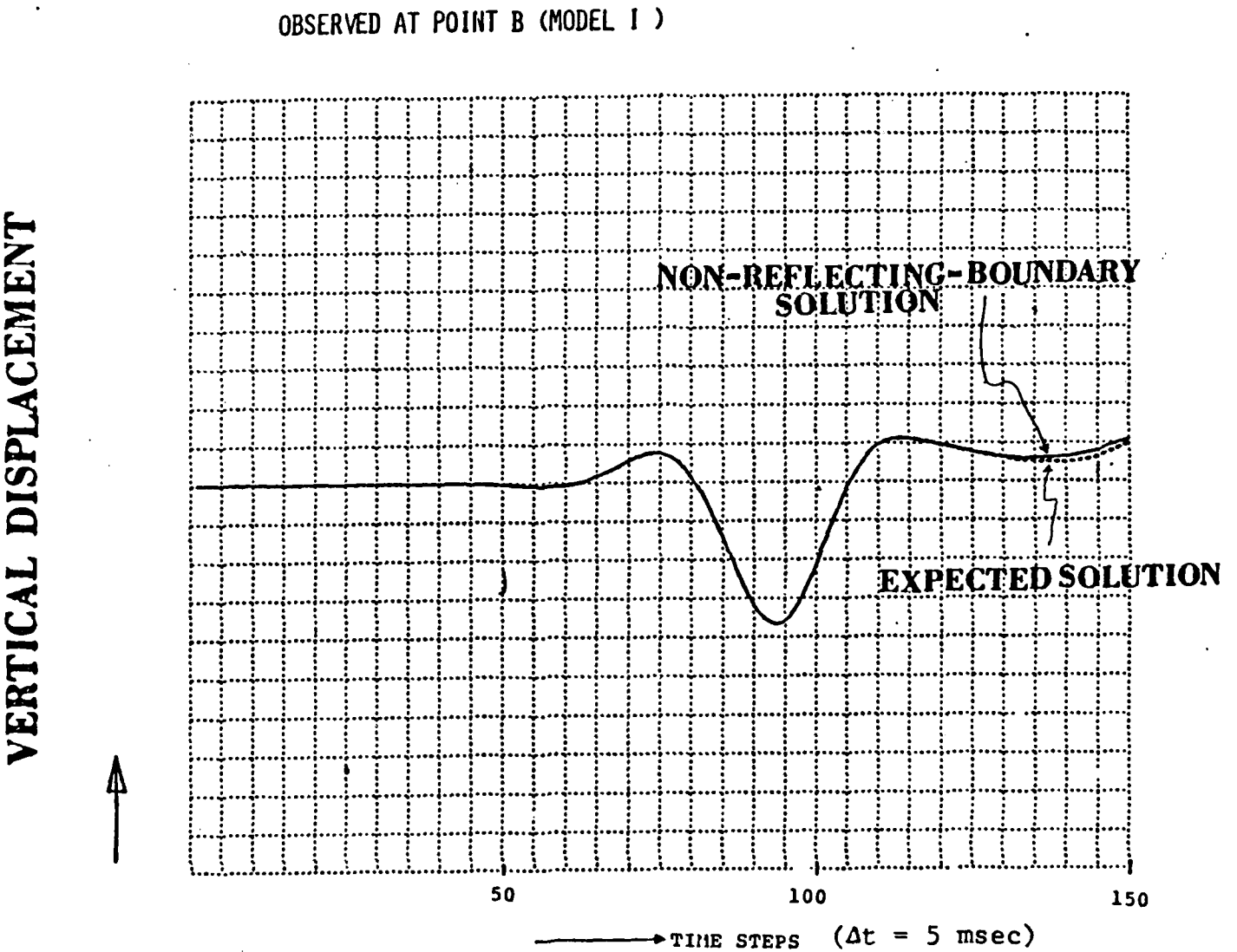

Figure 23a. Comparison of Vertical Displacements.

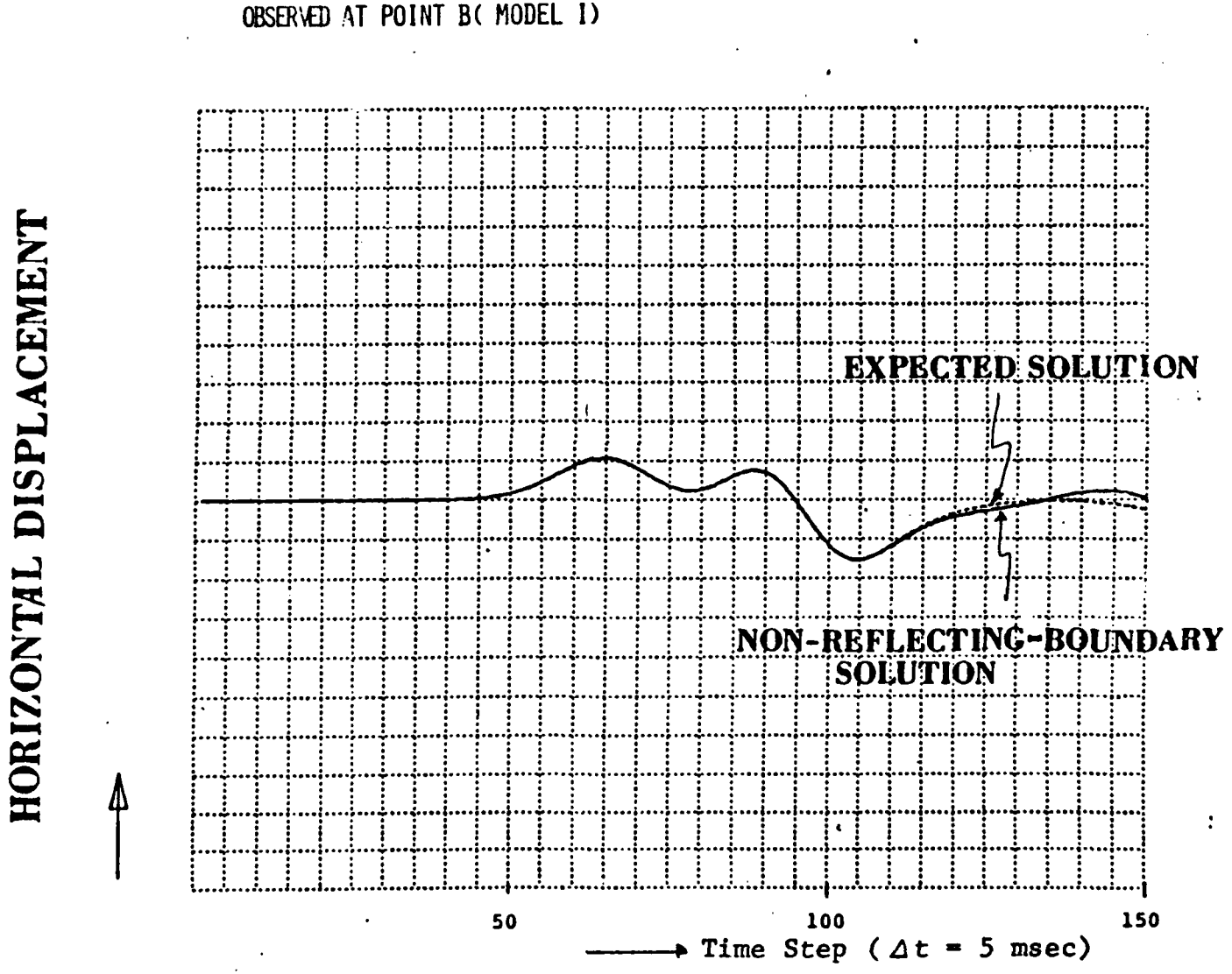

Figure 23b. Comparison of Horizontal Displacements.

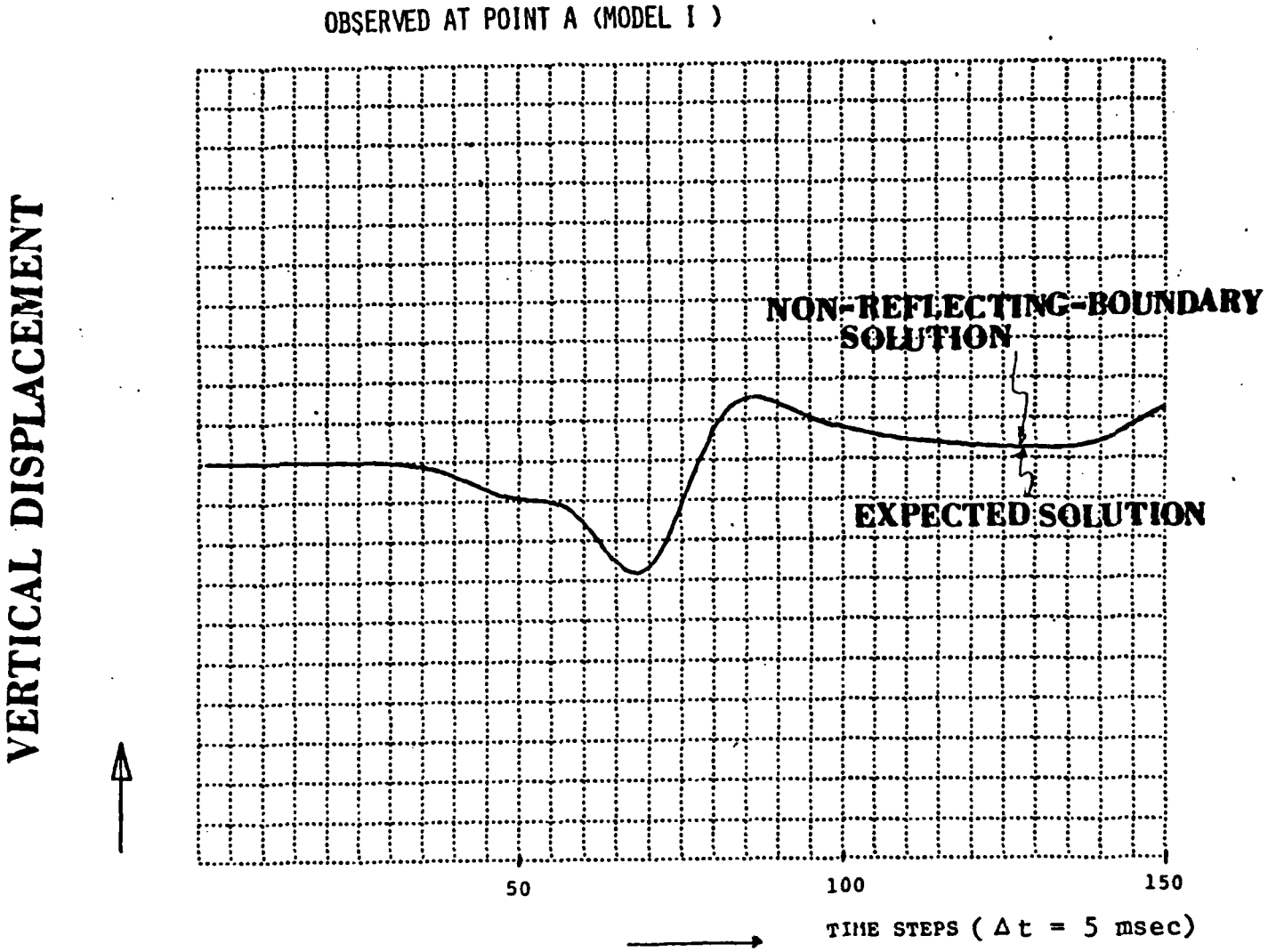

Figure 24a. Comparison of Vertical Displacements.

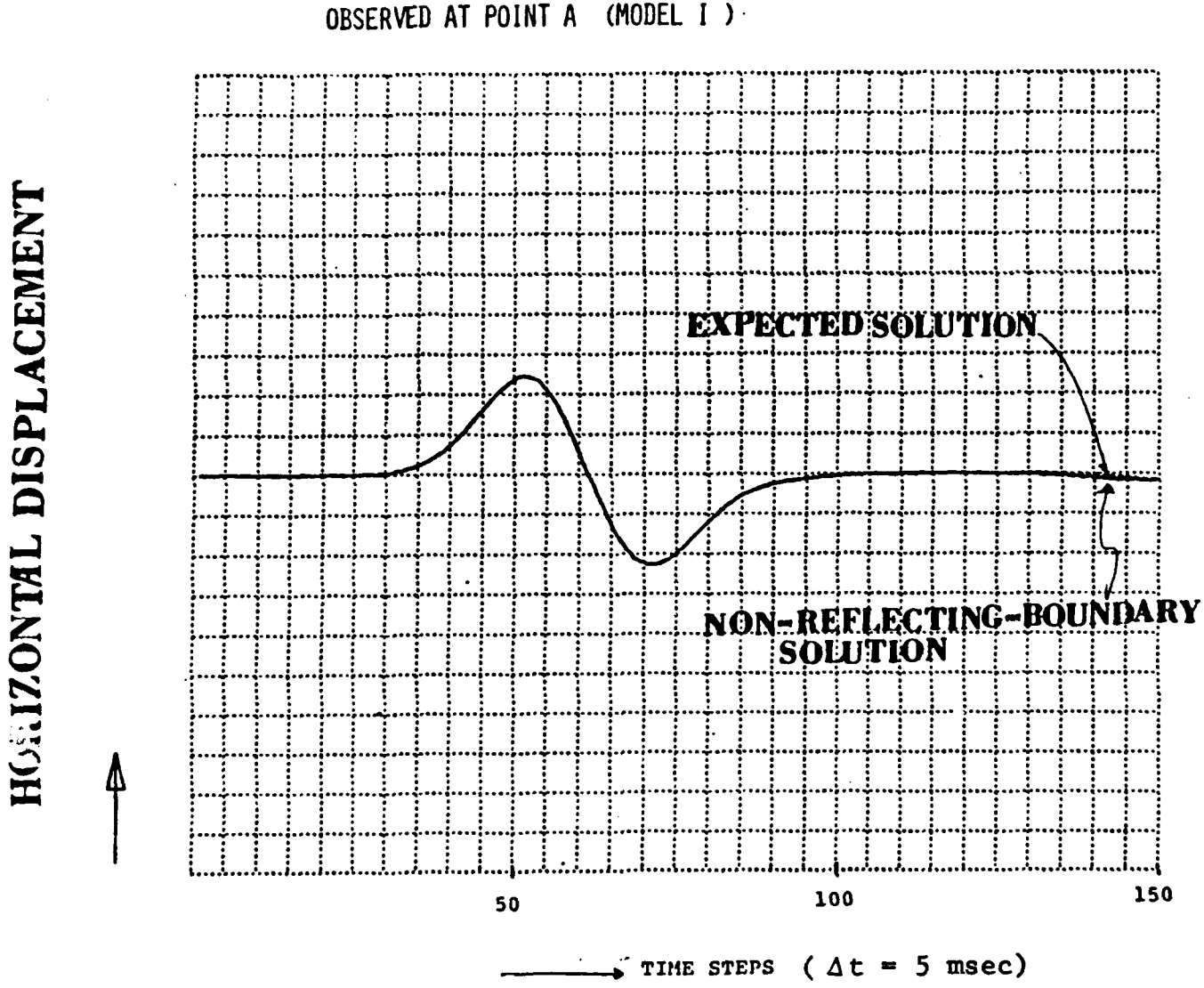

Figure 24b. Comparison of Horizontal Displacements.

Example 2:

In Example 1 we demonstrate the effect of using non-reflecting boundary conditions on one single boundary. Now, in this second example, non-reflecting boundary conditions are applied to two boundaries. The model is a half-space with the same elastic medium as Example 1 above with an internal source (Fig. 25a). Again, only half-size of the problem is needed to obtain the required solutions due to symmetry (Fig. 25b). Two models of different sizes are constructed: The large one (60 x 60 elements) generates the expected solutions; the small one (20 x 20 elements) is to test the non-reflecting effect. The small model contains only OABC. Figs. 26a and 26b show the responses as observed at corner C (see Fig. 25), the expected responses which are obtained by using the large model containing OA'B'C', and the solutions which are obtained by using the small model in which both AC and BC are imposed with free boundary conditions. It is evident that the expected solutions for both vertical and horizontal components do not agree with the traction-free boundary solutions. Analytically, corner C is singular. However, in the finite element algorithm, the non-reflecting boundary conditions based on modified Smith superposition method can be successfully applied to point C. Figs. 27a and 27b show the agreements between the above expected solutions and the non-reflecting boundary solutions. Again, this non-reflecting technique fails when a given wave is reflected at either boundary of AC and BC more than once.

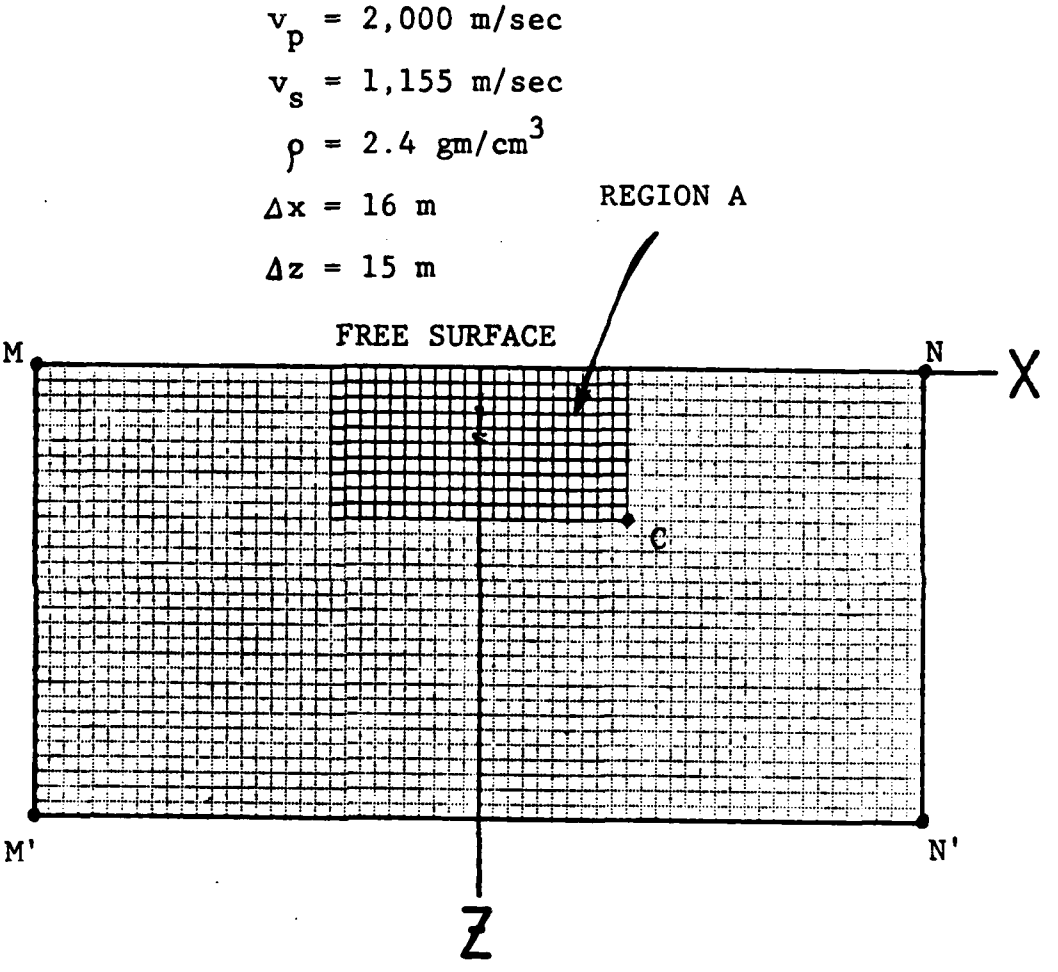

FINITE ELEMENT MODEL II

Figure 25a. Finite Element Model for an Elastic Half-Space. (Region A is the simulated half-space with the use of non-reflecting boundaries.)

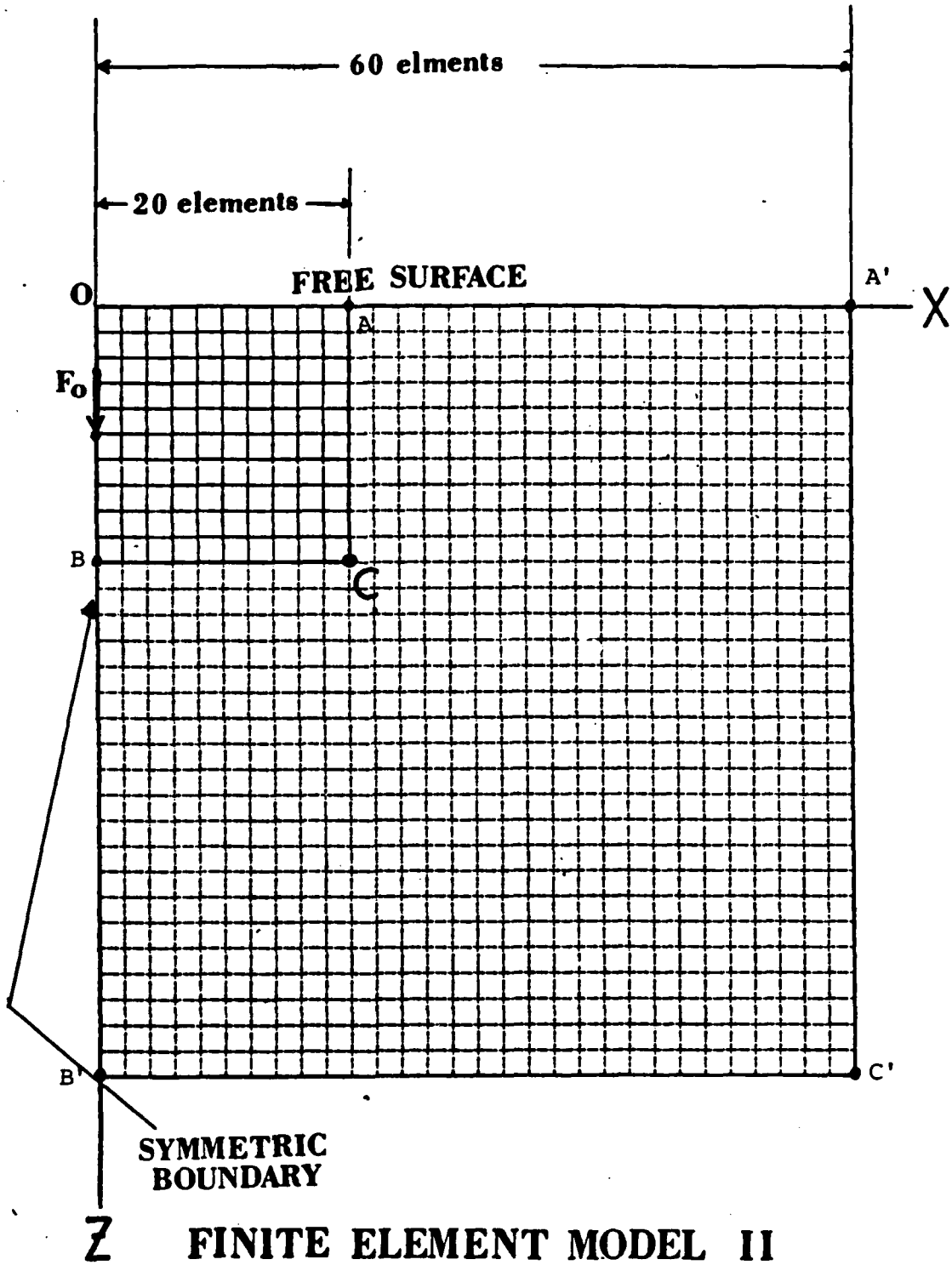

Figure 25b. Finite Element Mesh for an Elastic Half-Space with the Use of the Symmetric Boundary Conditions.

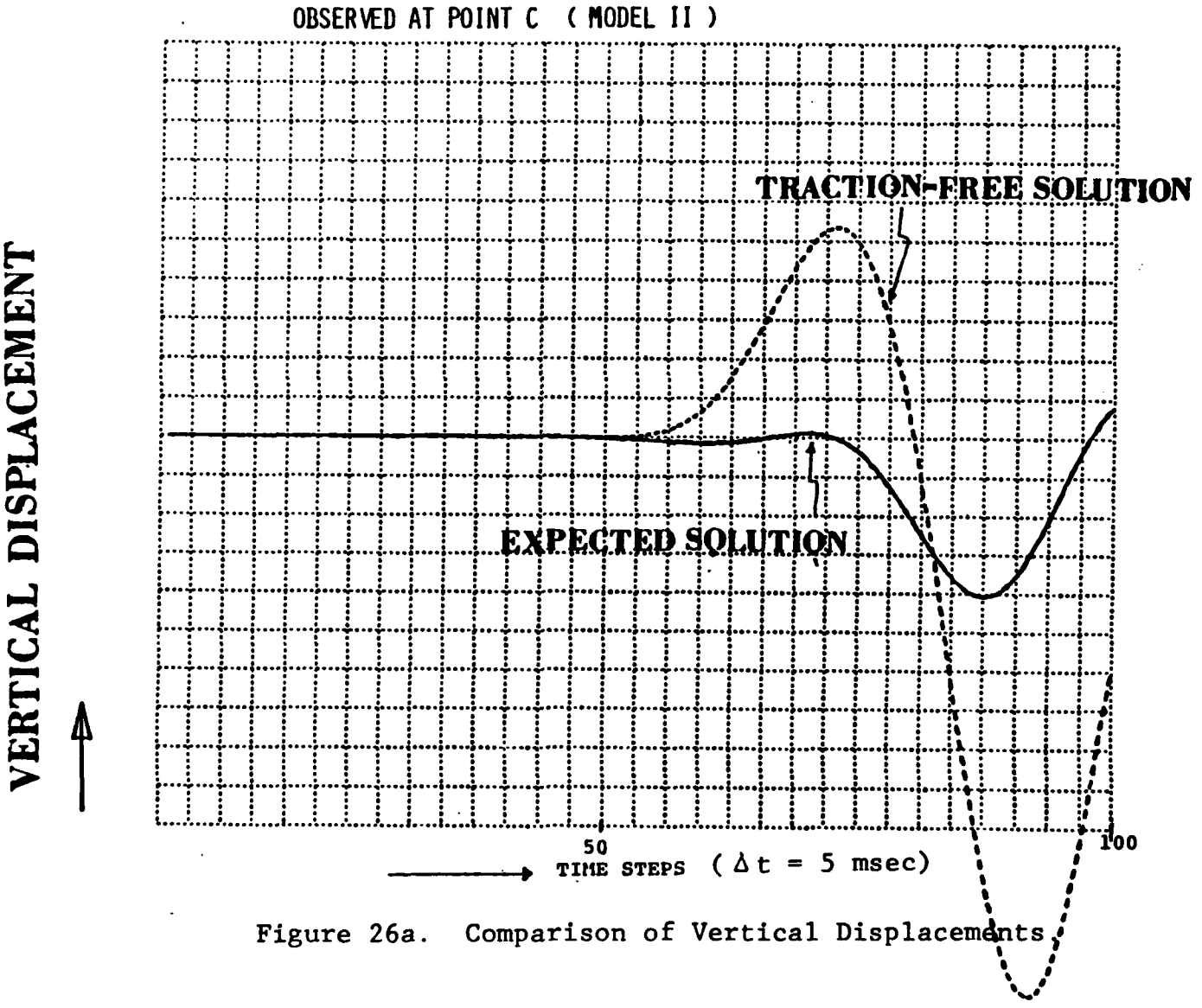

Figure 26a. Comparison of Vertical Displacements

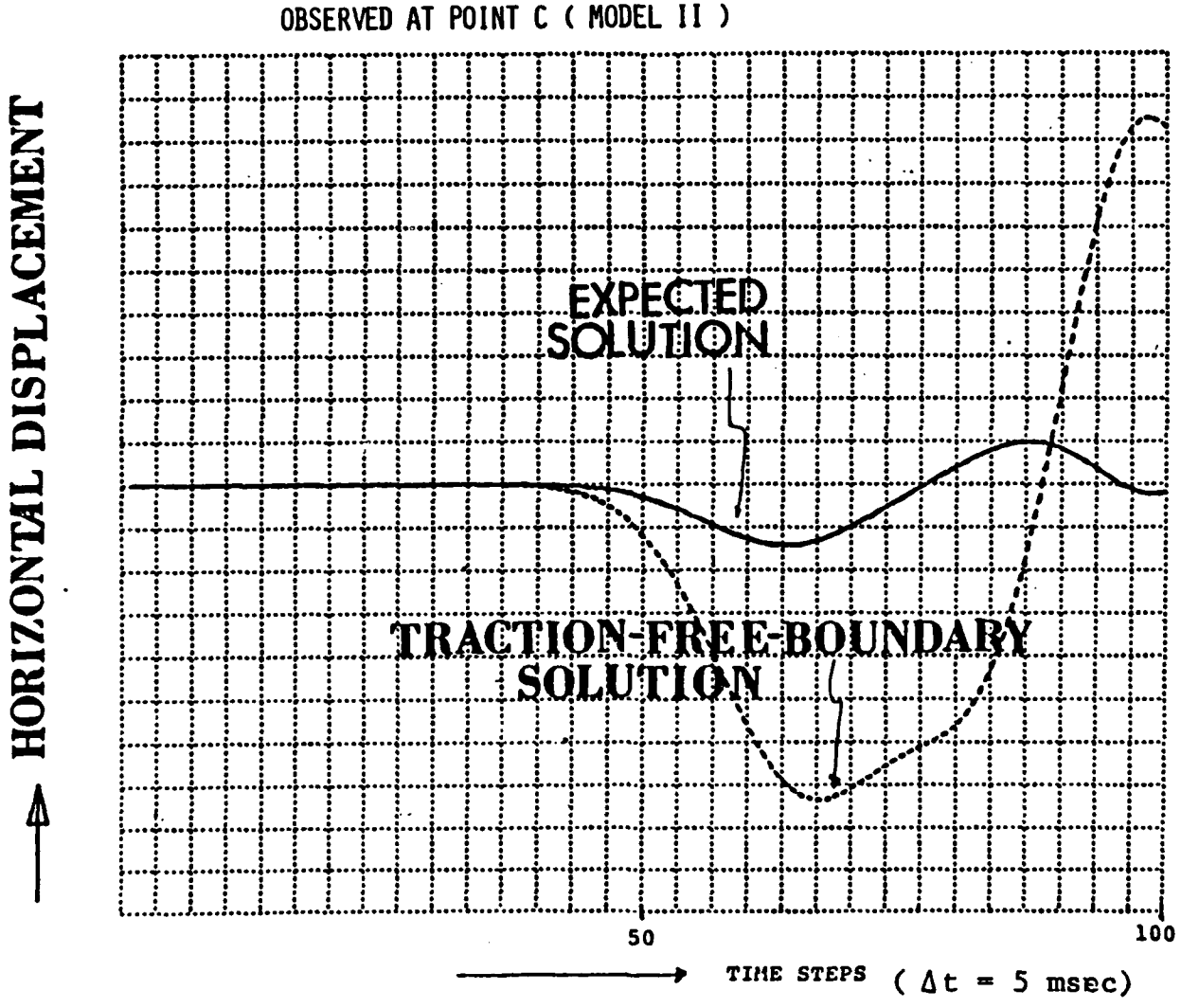

Figure 26b. Comparison of Horizontal Displacements.

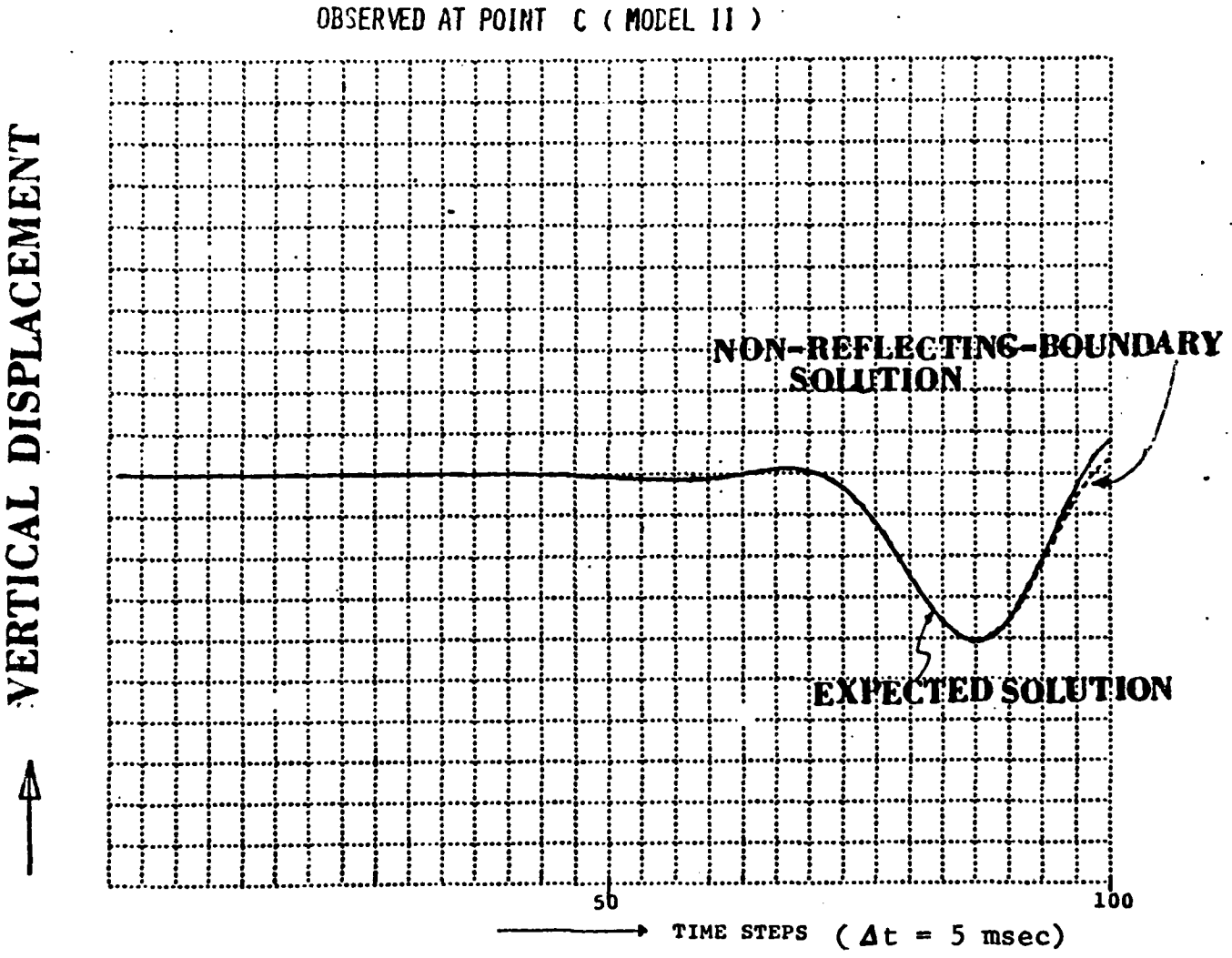

Figure 27a. Comparison of Vertical Displacements.

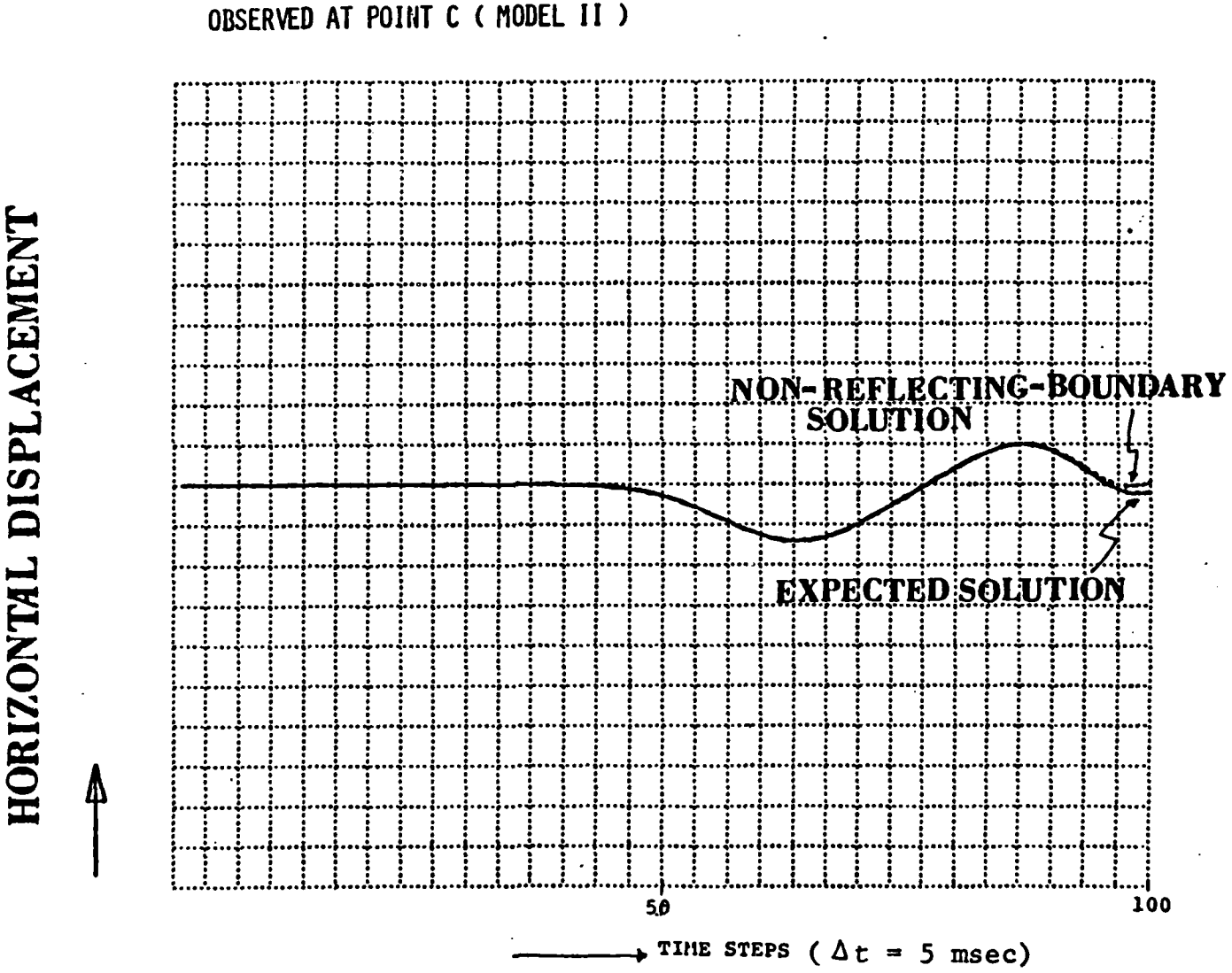

Figure 27b. Comparison of Horizontal Displacements.

(b) Effective Excitation (EE) Method

As mentioned in the Final Report of Contract F49620-77 -C-0130, "Elastic and Visco-Elastic Wave Scattering and Diffraction" (1977-1980), we used the direct step-ty-step explicit central-difference time integration scheme in AFEA3. Consequently, when the structure is subjected to an external disturbance, only the neighborning nodal points of the source are primarily excited while all other nodal points remain virtually undisturbed. The region of excitation motion expands with increasing time steps. For instance, we first consider a two-dimensional finite element mesh as shown in Fig. 28. If the source is located at point S, for the first time step we need only (i) to calculate the displacements, velocities, accelerations of those nodal points within the area $A_1B_1C_1D_1$, including the nodal points, and only (ii) to assemble the stiffness and mass matrices for those elements within the area $A_2B_2C_2D_2$. For the second time step, only those nodal points within the areas $A_1B_1C_1D_1$ and $A_2B_2C_2D_2$ and the elements within the area $A_3B_3C_3D_3$ are effectively excited, and so on. The same concept can be generalized to the three-dimensional case. In the Aldridge preliminary two-dimensional finite element code AFEA, the displacements, velocities, accelerations for every nodal point must be calculated for every time step. Consequently, the EE-method saves a large amount of computing time in the early stage of computation particularly for large finite element models.

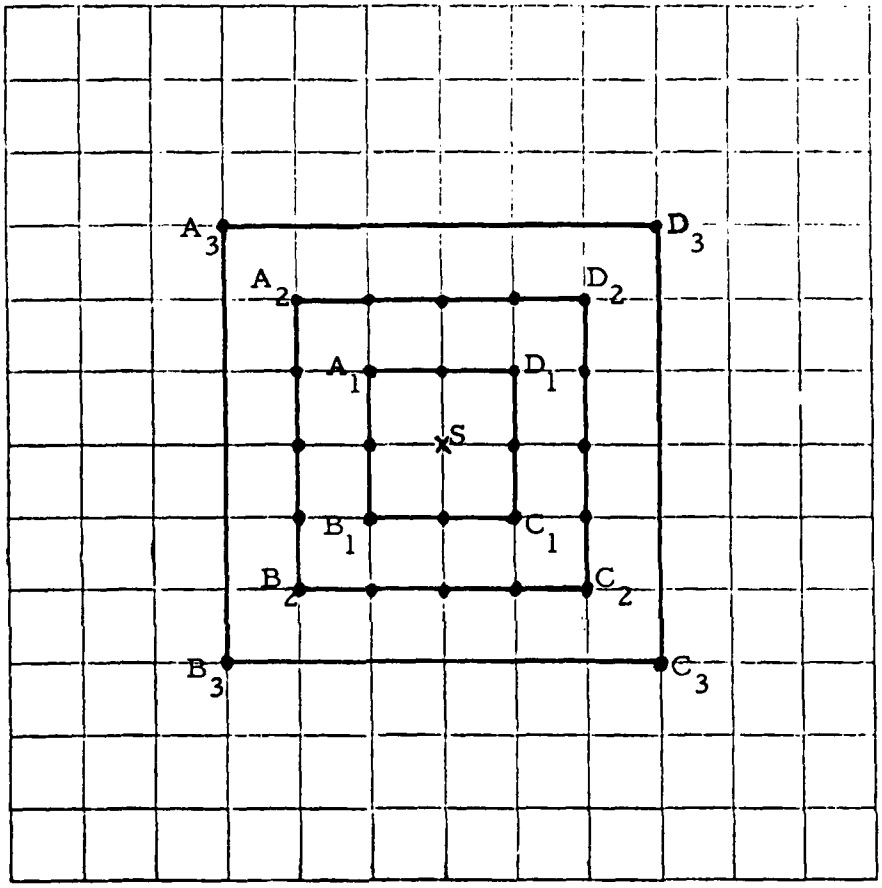

Figure 28. Two Dimensional Effective Excitation Finite Element Mesh.

(c) Introducing Relative Coordinates of the Nodal Points

In the old version of the AFEA, the mesh generator generates the value of the coordinates of the four nodal points of each quadrilateral, either a 4-CST (Constant Strain Triangles) or an averaging 2-CST quadrilateral, element with respect to the global system (Fig. 29)

AX(n), BX(n), CX(n), DX(n)

AX(n), BY(n), CY(n), DY(n)

where n = 1, 2, 3, ... N, N is the number of total elements. Thus, we require incore storage with a number of 8 x N words for the eight variables. Actually, we need only assign the relative coordinates of one element since we are dealing with regular size element temporarily. The introduction of the relative coordinates is based on the fact that both the shape function [N] and the strain-displacement matrix [B] of the triangle elements depend on the relative coordinates of the element only. Thus, in the new version of AFEA, we need only eight incore words for these eight variables.

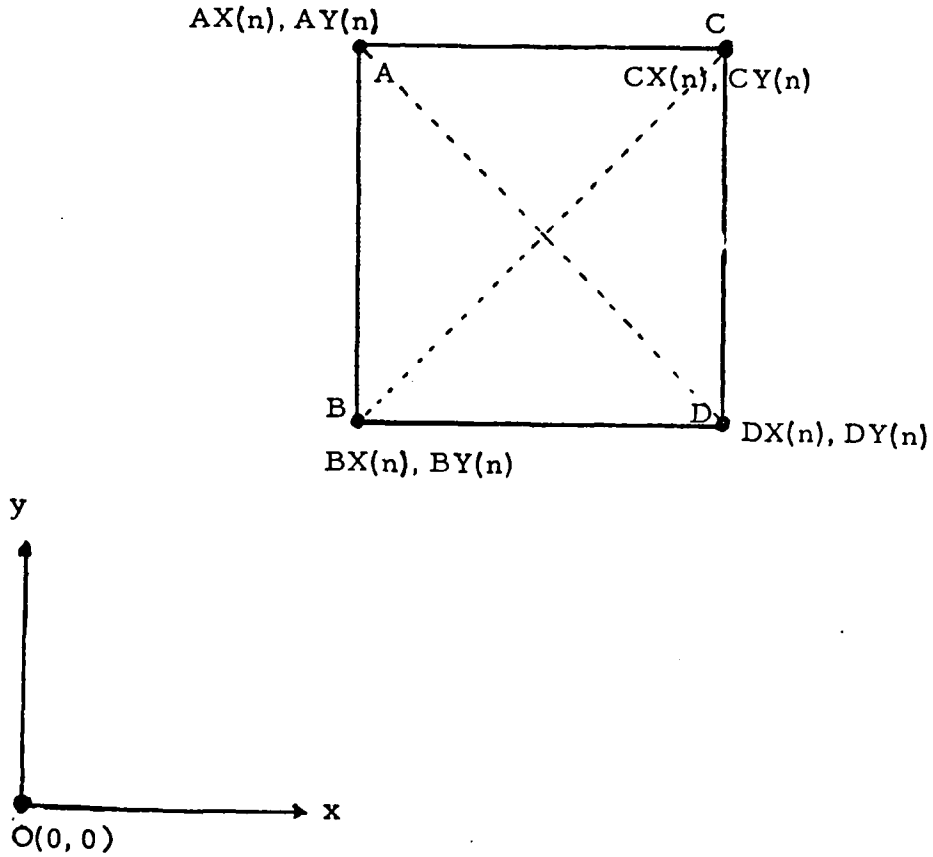

Figure 29. The Coordinates of the n^{th} Element.

(d) Restart Back-Up Option

In the new version of the two-dimensional computer code, we have included a restart back-up option, that is, we save the displacements and velocities of every nodal point after a certain number of time steps. The new back-up results will overwrite on the same tape to replace the old back-up results. If the integer IFLAG has a number zero, the option will start from the beginning; any other numbers of IFLAG will mean that the option is restarted from where it last executed. This feature greatly facilitates effectiveness of computation in case of failure of the computer.

FUTURE RESEARCH

In the second year of the present contract, the research emphasis will be in the following three areas.

A. Continuing a systematic investigation of the finite element basin models.

B. Studying the finite element source mechanism.

C. Further improving the finite element computer codes.

* * *

A. Finite Element Basin Models

The models shown in Fig. 29 are proposed to be investigated. In Figs. 29b and 29c, various dip angles of 50°, 60°, and 70° will be considered.

As mentioned in Section II of this report, the center frequency of the source for our previous basin model studies is around 2 Hz. Responses for higher frequencies will be included in the coming year's research.

B. Finite Element Source Mechanism

In our previous finite element model study, we used either a line source for the case of SH wave propagation, or a directional forcing function for the elastic case. To simulate a point source for the elastic case has been a very challenging subject in finite element algorithm. Recently, we

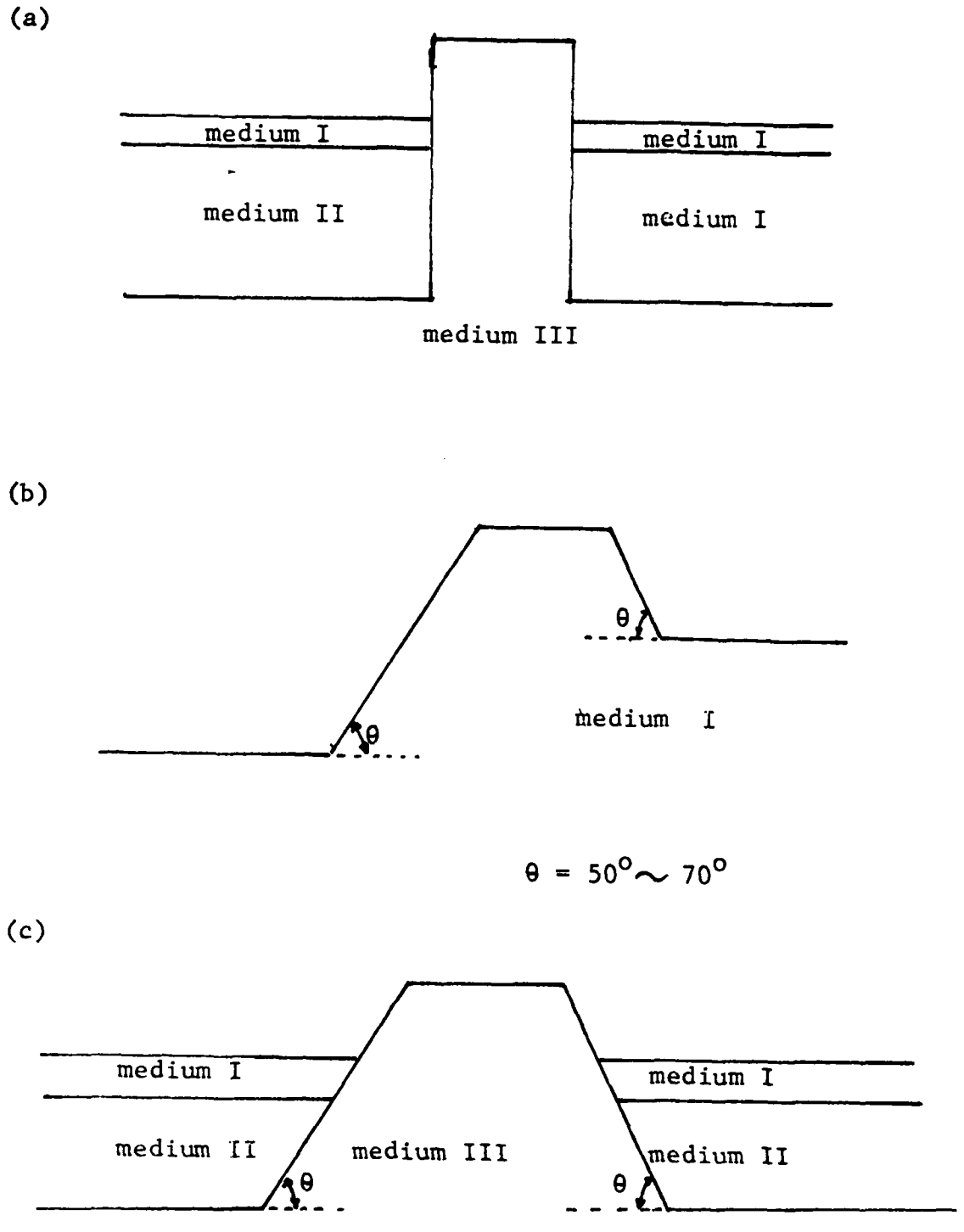

Figure 30. The Geometry of the Proposed Basin Models.

found that not only the point source but concentrated multipole sources can be simulated by using the energy-sharing-nodals technique. In the coming year we propose to investigate systematically the elastic half-space subjected to various loadings (couple, quadruple, double couple, and so on) for the elastostatic case and compare the finite element results with the analytical solutions. Once we have a thorough understanding of these aspects, we can then pursue a study of the equivalent elastodynamic case.

C. Modifying the Computer Codes

The basic problem which we face in the finite element modeling is still that of large storage for the dimensions required for high frequency studies. Further improvements are still needed so that a more realistic basin model can be tackled.

References

Kuo, J. T., Y. C. Teng, K. E. Chen, C. E. Shepherd, "Elastic and Viscoelastic Wave Scattering and Diffraction," Final Report of Air Force Contract F49620-77-0139, 1981.

Kuo, J. T., Y. C. Teng, "Ground Response in Alluvial Basins Due to Seismic Disturbances," First, Second, and Third Status Reports, 1981 and 1982.

Lysmer, L, R. L. Kuhlemeyer, "Finite Dynamic Model for Infinite Media," J. Eng. Mech. Div., ASCE, 95, 859-877, 1969.

Smith, W., "A Non-Reflecting Plane Boundary for Wave Propagation Problems," J. Comp. Phys., 15, 492-503, 1973.

END

FILMED

2-83

DTIC